Interference-induced magnetoresistance in HgTe quantum wells

I. V. Gornyi,[1,2] V. Yu. Kachorovskii,[1,2] and P. M. Ostrovsky[3,4]
[1]*Institut für Nanotechnologie, Karlsruhe Institute of Technology, 76021 Karlsruhe, Germany*
[2]*A.F. Ioffe Physico-Technical Institute, 194021 St. Petersburg, Russia*
[3]*Max-Planck-Institute for Solid State Research, D-70569 Stuttgart, Germany*
[4]*L. D. Landau Institute for Theoretical Physics RAS, 119334 Moscow, Russia*
(Received 22 April 2014; revised manuscript received 11 July 2014; published 1 August 2014)

We study the quantum interference correction to the conductivity in HgTe quantum wells using the Bernevig-Hughes-Zhang model. This model consists of two independent species (blocks) of massive Dirac fermions. We describe the crossover between the orthogonal and symplectic classes with increasing the carrier concentration and calculate, respectively, weak localization and antilocalization corrections in the absence of the block mixing and assuming the white-noise disorder within each block. We have calculated the interference-induced magnetoresistance in a wide interval of magnetic fields, in particular, beyond the diffusion regime. Remarkably, each Dirac cone taken separately gives a linear contribution to the low-field magnetoresistance, which turns out to be asymmetric in magnetic field B. We present an interpretation of this result in terms of the Berry-phase formalism. The contributions of the two blocks are related to each other by replacing B to $-B$, so that the total magnetoresistance is symmetric and parabolic in the limit $B \to 0$. However, in some range of parameters, field dependence turns out to be strongly nonmonotonous. We also demonstrate that block mixing gives rise to additional singular diffusive modes which do not show up in the absence of mixing.

DOI: 10.1103/PhysRevB.90.085401 PACS number(s): 73.20.Fz, 72.20.Dp, 75.47.−m

I. INTRODUCTION

It is well known that the low-temperature transport in disordered systems is crucially affected by quantum interference effects. The first-order term in a series expansion of the conductivity in $1/k_F l$ (here k_F is the Fermi wave vector and l is the mean-free path) contains the weak localization (WL) correction [1] (for a review, see Ref. [2]). The underlying physics is the coherent enhancement of the backscattering amplitude which comes from the constructive interference of the waves propagating in the opposite directions (clockwise and counterclockwise) along a closed loop formed by scatterers (see Figs. 1 and 2). A remarkable feature of this correction is the logarithmic divergence at low temperatures in the two-dimensional (2D) case. Such a divergency is a precursor of the strong localization effects and, therefore, reflects universal symmetry properties of the system. An external magnetic field breaks the time-reversal symmetry and, as a consequence, leads to a suppression of the WL correction. On the other hand, spin-orbit coupling does not violate the time-reversal symmetry, but strongly modifies the quantum conductivity correction because of the interference of the spin parts of the waves. In particular, strong spin-orbit coupling leads to a destructive interference [3] between clockwise- and counterclockwise-propagating paths, thus changing the sign of the quantum correction. The change from the WL to the weak antilocalization (WAL) behavior was considered for the first time in Ref. [3] and was further addressed, both theoretically and experimentally, in a number of more recent papers (see Refs. [4–31] and references therein).

Recently, the interest in quantum transport in the systems with strong spin-orbit coupling dramatically increased after the discovery that such systems may exhibit a topological insulator (TI) phase [32–38] with preserved time-reversal invariance. In the 2D case, the TI behavior was predicted by Bernevig, Hughes, and Zhang (BHZ) [34] for HgTe/HgCdTe quantum wells (QWs). Soon after this prediction, the existence of a TI phase was experimentally demonstrated in Refs. [35,39] in HgTe/HgCdTe QWs with band inversion. The latter resulted in emergence of delocalized (topologically protected) helical modes at the edge of the sample. Another realization of a 2D TI based on InAs/GaSb structures was proposed in Ref. [40] and was experimentally discovered in Ref. [41].

When the Fermi energy in a HgTe/HgCdTe QW is shifted away from the band gap, the system exhibits a 2D metallic phase known as a 2D spin-orbit metal (SOM). The spectrum of the SOM can be well approximated by the Dirac spectrum of massive fermions (with the mass proportional to the band gap), so that the quantum transport in such a system is strongly affected by the Dirac nature of carriers [42–47] and, owing to the presence of the Berry phase, bears certain similarity to interference phenomena in graphene [48–51], in 2D semiconducting hole structures [31,52], and in surface layers of 3D TI [42,53,54].

The remarkable property of the 2D SOM is the dependence of the effective spin-orbit coupling on the particle concentration. For low concentration, the spectrum is approximately parabolic, while the coupling is weak and can be neglected in the first approximation. Then, the system belongs to so-called orthogonal symmetry class and one can expect conventional WL behavior of the quantum correction. On the other hand, at large concentrations, when the Fermi energy becomes much larger than the gap width, the spectrum is quasilinear, while the spin is strongly coupled to the particle momentum, so that the underlying symmetry class is symplectic and the SOM would demonstrate WAL similar to graphene-based structures. Recently, the magnetoresistivity of HgTe/HgCdTe structures was experimentally studied away from the insulating regime in Refs. [55–58], both for inverted and normal band ordering. The experiments demonstrate that the system may show both WL and WAL behavior. Hence, there is a clear need in a theory which can rigorously describe the crossover

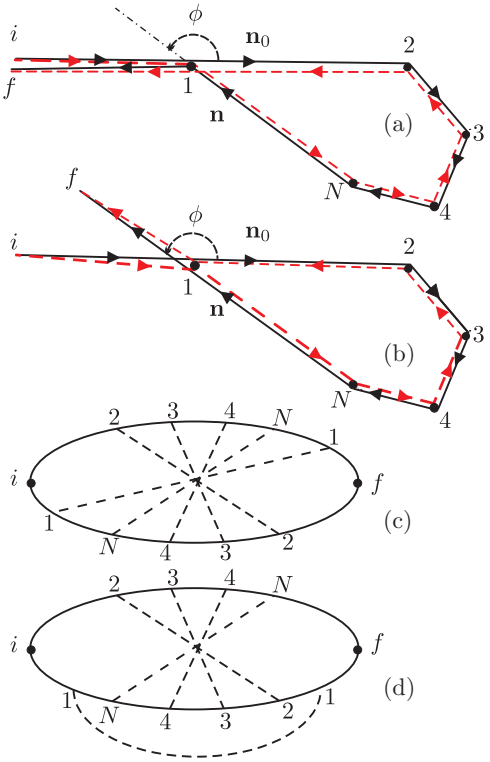

FIG. 1. (Color online) Backscattering (a) and nonbackscattering (b) scattering processes on a complex of impurities consisting of $1,2,\ldots,N$ impurities and corresponding diagrams (c) and (d).[For simplicity, we do not show in (a) and (b) diffusive motion of the particle before and after the loop. Such motion leads to "transportization" of vertexes i and f.]

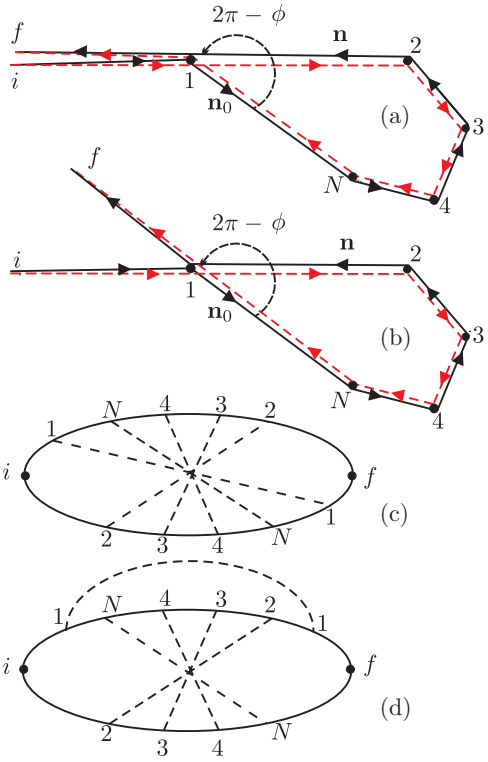

FIG. 2. (Color online) The processes (a), (b) and corresponding diagrams leading to the contribution which is complex conjugated to the one given by the processes shown in Fig. 1.

between the two symmetry classes that correspond to WL and WAL regimes.

A theoretical study of the quantum transport in the 2D SOM in HgTe/HgCdTe QWs was undertaken in Ref. [43] for the case when the chemical potential is located in the almost linear range of the spectrum. The conductivity correction was calculated within the diffusive approximation. The WAL nature of the correction was demonstrated and attributed to the Berry-phase mechanism characteristic of the Dirac systems. It was also shown that the weak nonlinearity of the dispersion (due to a finite band gap) suppresses the quantum interference on large scales. Another approach to the problem based on the analysis of the symmetry properties of the underlying Dirac-type Hamiltonian and physically important symmetry-breaking mechanisms was proposed in Ref. [44]. This approach captures the universal properties of the system and, consequently, allows one to find without microscopic calculations the singular (logarithmic in 2D) interference corrections within the diffusion approximation. This approximation is sufficient near the band bottom and in the regime of almost linear spectrum for relatively weak magnetic fields. The ballistic case was discussed in Ref. [45] for zero magnetic field. Also, the quantum transport in HgTe/HgCdTe QWs was numerically simulated both in the ballistic and diffusive samples in Ref. [46] where the influence of the Berry phase (similar to the effect of Berry phase in semiconducting hole structures [52]) on magnetoresistance was emphasized.

In this paper, we present a systematic analysis of the interference corrections in a 2D SOM biased by gate away from the TI regime. Having in mind to describe the crossover between two symmetry classes we generalize the approach of Ref. [45] for nonzero magnetic fields and develop a ballistic theory of the quantum transport valid beyond the diffusion approximation and, therefore, applicable for a wide range of particle concentrations.

We start with discussing the basic equations and properties of such a SOM (see Sec. II). As a starting model, we will use BHZ Hamiltonian [34], which allows one to describe TI in a wide range of particle concentration both in the normal and in the inverted states. We discuss the dependence of the conductivity correction on key parameters of the model. Although our theory is valid for a wide range of parameters, in order to simplify intermediate calculations we will use the simplified version of this model which corresponds to two equivalent massive Dirac cones with momentum-independent mass and velocity.

Next, we derive a kinetic equation for the Cooperon propagator within a single cone and find its exact solution valid beyond the diffusion approximation (see Sec. III). In Sec. IV, we use these results to evaluate the interference corrections in a wide interval of electron concentration and magnetic fields, assuming that two equivalent blocks of the system (BHZ blocks) are not mixed by any perturbation. One of the main results of this section is the demonstration of the strong asymmetry (with respect to the inversion of the sign of the magnetic field) of the contribution of a single block. This result can be explained within the Berry-phase

formalism and turns out to be in a good agreement with the previous numerical simulations [46]. Summing of the contributions of two blocks restores symmetry with respect to the field inversion. However, field dependence turns out to be strongly nonmonotonous in some range of the parameters. We also predict a nonmonotonous dependence of the quantum correction on the phase-breaking rate. Similar result was predicted earlier for weak localization of holes in conventional heterostructures [31].

In Sec. V, we generalize obtained results assuming that blocks are weakly coupled to each other. Most interestingly, the block mixing gives rise to additional singular diffusive modes which do not show up in the absence of mixing. One of these modes is a "purely singular" mode which is responsible for the WAL at very low temperatures. Existing of such singular modes leads to an additional mechanism of the nonmonotonous magnetoresistance.

In the end of the paper, we present plots demonstrating dependence of the interference correction on different parameters (see Sec. VI). We also discuss asymptotical behavior of the quantum correction in the strong-field limit (see Sec. VI E). In this limit, the main contribution to the correction is given by scattering on complexes of three impurities separated by untypical distances much smaller than the mean-free path (for discussion of such an asymptotic in the parabolic spectrum, see Refs. [59,60]). Technical details of the calculations are placed in Appendices A–E.

II. BASIC EQUATIONS

A. BHZ Hamiltonian

The effective Hamiltonian for a narrow symmetric HgTe quantum well (QW) was derived by Bernevig, Hughes, and Zhang (BHZ) in Ref. [34] in the framework of the $\mathbf{k}\cdot\mathbf{p}$ method. The BHZ Hamiltonian has a 4×4 matrix structure in the spin (sign of the z projection of the total momentum $\mathbf{J}$, where the z axis is perpendicular to the QW plane) and E1-H1 ($|J_z|=\frac{1}{2}$ and $|J_z|=\frac{3}{2}$ bands, respectively) space,

$$H_{\rm BHZ}=\begin{bmatrix} H_{\rm I}(\mathbf{k}) & 0 \\ 0 & H_{\rm II}(\mathbf{k})\end{bmatrix}, \tag{1}$$

where

$$H_{\rm I}(\mathbf{k})=\begin{bmatrix} \epsilon(\mathbf{k})+m(\mathbf{k}) & v(k_x+ik_y) \\ v(k_x-ik_y) & \epsilon(\mathbf{k})-m(\mathbf{k})\end{bmatrix} \tag{2}$$

and

$$H_{\rm II}(\mathbf{k})=H_{\rm I}^{*}(-\mathbf{k})=\begin{bmatrix} \epsilon(\mathbf{k})+m(\mathbf{k}) & -v(k_x-ik_y) \\ -v(k_x+ik_y) & \epsilon(\mathbf{k})-m(\mathbf{k})\end{bmatrix}. \tag{3}$$

Here, we have used the form given in Refs. [33,40] with the following arrangement of components in the spinor: $E1+, H1+, E1-, H1-$.

The functions $\epsilon(\mathbf{k})$ and $m(\mathbf{k})$ are effective energy and mass which are assumed to be isotropic in the momentum space. Within the $\mathbf{k}\cdot\mathbf{p}$ expansion in the vicinity of the Γ point, they are given by

$$\epsilon(\mathbf{k})=C+D\mathbf{k}^2, \quad m(\mathbf{k})=mv^2+B\mathbf{k}^2. \tag{4}$$

We note that, in general, v might also depend on $\mathbf{k}$ [61].

The two phases of normal and topological insulator correspond to $m>0$ and $m<0$, respectively. The sign of m changes at the critical thickness d_c of the QW of about 6.2 nm [35]. The quantities B and D are positive with $B>D$. The parameter C can be eliminated by a shift of the chemical potential.

As seen from Eq. (1), the Hamiltonian $H_{\rm BHZ}$ breaks up into two blocks acting independently in the spin-up and spin-down subspaces. The blocks have the same spectrum

$$E^{\pm}_{\mathbf{k}}=\epsilon(\mathbf{k})\pm\sqrt{v^2k^2+m^2(\mathbf{k})}. \tag{5}$$

The eigenfunctions for each block are two-component spinors in E1-H1 space:

$$\psi^{(\pm)}_{\mathbf{k}}(\mathbf{r})=\chi^{(\pm)}_{\mathbf{k}}\,e^{i\mathbf{kr}}. \tag{6}$$

The spinors $\chi^{(\pm)}_{\mathbf{k}}$ are different in different blocks:

$$\chi^{(\rm I,+)}_{\mathbf{k}}=\frac{1}{\sqrt{1+\eta}}\begin{pmatrix}1\\ \sqrt{\eta}e^{-i\phi_{\mathbf{k}}}\\ 0\\ 0\end{pmatrix}, \tag{7}$$

$$\chi^{(\rm I,-)}_{\mathbf{k}}=\frac{1}{\sqrt{1+\eta}}\begin{pmatrix}-\sqrt{\eta}e^{i\phi_{\mathbf{k}}}\\ 1\\ 0\\ 0\end{pmatrix}, \tag{8}$$

$$\chi^{(\rm II,+)}_{\mathbf{k}}=\frac{1}{\sqrt{1+\eta}}\begin{pmatrix}0\\ 0\\ 1\\ -\sqrt{\eta}e^{i\phi_{\mathbf{k}}}\end{pmatrix}, \tag{9}$$

$$\chi^{(\rm II,-)}_{\mathbf{k}}=\frac{1}{\sqrt{1+\eta}}\begin{pmatrix}0\\ 0\\ \sqrt{\eta}e^{-i\phi_{\mathbf{k}}}\\ 1\end{pmatrix}, \tag{10}$$

with $\phi_{\mathbf{k}}$ being the polar angle of the momentum $\mathbf{k}$ and

$$\eta=\eta(k)=\left[\frac{vk}{m(\mathbf{k})+\sqrt{v^2k^2+m^2(\mathbf{k})}}\right]^2. \tag{11}$$

Parameter η is the key quantity of the problem. At temperatures smaller than the Fermi energy one may replace k with k_F, so that we put throughout the paper

$$\eta=\eta(k_F). \tag{12}$$

This parameter is the function of the particle concentration.

As we will see in the following, η governs the crossover from WL to WAL. In particular, in the absence of dephasing processes and for zero magnetic field, the conductivity correction depends on η only: $\delta\sigma=\delta\sigma(\eta)$, so that all essential information about the particular dependencies $m(\mathbf{k})$ and $v(\mathbf{k})$ is encoded in η, while the specific dependence $\epsilon(\mathbf{k})$ drops out from the resulting equations [62]. It is worth stressing that η is the same for two spectrum branches [see Eq. (5)]. This implies that the electron and hole conductivity corrections coincide (for a given value of k_F). Moreover, as we will see in the following, the dependence of the correction on η obeys an essential property $\delta\sigma(\eta)=\delta\sigma(1/\eta)$. As follows from Eq. (11), this property ensures that inversion of sign of the mass $m(k_F)\to -m(k_F)$ does not change the correction.

In other words, conductivity corrections for normal material with the mass $m(k_F) > 0$ and inverted material with the mass $-m(k_F)$ are equal. This allows us to limit our consideration to the normal case and upper branch of the spectrum. In this case,

$$0 \leqslant \eta \leqslant 1.$$

We will see that for $\eta \to 0$ the quantum correction is negative (weak localization), while for $\eta \to 1$, the sign of the quantum correction changes (weak antilocalization). Hence, with changing the electron (hole) concentration, the system undergoes a transition between orthogonal and symplectic classes.

In a more general case, when magnetic field is applied perpendicular to the quantum well plane and dephasing processes are taken into account, the conductivity correction is expressed in terms of three parameters (here we neglect block mixing):

$$\delta\sigma = \delta\sigma\left(\eta, \frac{l}{l_B}, \frac{\tau}{\tau_\phi}\right), \tag{13}$$

where τ and $l = v_F\tau$ are the mean-free time and mean-free path at the Fermi level, respectively, $v_F = |(\partial E_{\mathbf{k}}/\partial k)_{k=k_F}|$ is the Fermi velocity, l_B is the magnetic length, and τ_ϕ is the phase-breaking time. This equation is valid for both spectrum branches [which, in general, have slightly different l and τ/τ_ϕ for fixed k_F due to the term $\epsilon(\mathbf{k})$] and is invariant under replacement: $m(k_F) \to -m(k_F)$, $\eta \to 1/\eta$ (one can check that τ, l, and v_F are invariant under this replacement). Therefore, the symmetry with respect to mass inversion $m(k_F) \to -m(k_F)$ still holds.

Although our results are valid for general Hamiltonian (1) with arbitrary parameters B, C, and D, in what follows, in order to simplify intermediate calculations, we will consider the simplified model with $B = C = D = 0$.

B. Single massive Dirac cone

Having in mind symmetry arguments presented in the previous section, we only consider normal case with the positive mass. We assume that the Fermi level lies outside the gap in the region of the positive energies, thus focusing on the upper branches of the spectrum in both blocks. We start with the discussion of the properties of a single block (for definiteness, the block II). The contribution of the other block and the effects caused by the interblock transitions will be considered in Secs. IV B and V, respectively.

In the framework of the simplified model with $B = C = D = 0$, the expressions for the spectrum and the wave functions simplify:

$$E_{\mathbf{k}} = \sqrt{m^2v^4 + v^2k^2}, \tag{14}$$

$$\chi_{\mathbf{k}} = \frac{1}{\sqrt{1+\eta}}\begin{pmatrix} 0 \\ 0 \\ 1 \\ -\sqrt{\eta}e^{i\phi_{\mathbf{k}}} \end{pmatrix}, \tag{15}$$

$$\eta = \left(\frac{k}{mv + \sqrt{m^2v^2 + k^2}}\right)^2. \tag{16}$$

Within this approximation, $\eta \to 0$ for low concentration in the region of the parabolic spectrum and $\eta \to 1$ for large concentrations when the Fermi energy is large compared to the band gap and the spectrum is quasilinear. The Fermi velocity, density of states (per block), Fermi energy, and Fermi momentum are expressed explicitly in terms of η as follows:

$$v_F = \frac{2\sqrt{\eta}}{1+\eta}v, \quad \nu_F = \frac{m}{2\pi\hbar^2}\frac{1+\eta}{1-\eta}, \tag{17}$$

$$E_F = mv^2\frac{1+\eta}{1-\eta}, \quad k_F = \frac{2mv}{\hbar}\frac{\sqrt{\eta}}{1-\eta}. \tag{18}$$

Importantly, the particular dependence of these quantities on η enters only the last two arguments in Eq. (13), l/l_B and τ/τ_ϕ. At the same time, the explicit dependence of $\delta\sigma$ on η arises solely from the spinor structure of the wave functions and hence is not specific for the model with $B = C = D = 0$.

The standard way [43] to introduce disorder in the model is to add the fully diagonal term

$$H_{\text{dis}} = V(\mathbf{r})\hat{I}, \tag{19}$$

with a random potential $V(\mathbf{r})$ to the effective Hamiltonian H_{BHZ} (here $\hat{I}$ is unit 4×4 matrix). While the diffusive behavior of the quantum interference correction is universal, the precise from of the correction in the ballistic regime depends on the particular form of the disorder correlation function. We will assume the white-noise disorder with the correlation function

$$\langle V(\mathbf{r})V(\mathbf{r}')\rangle = W\delta(\mathbf{r} - \mathbf{r}'). \tag{20}$$

As usual for the weak localization (antilocalization) regime, we assume that $k_Fl \gg 1$ and $E_F\tau \gg 1$ that allows us to neglect mixing of the upper and lower branches. Then, the matrix Green's function can be written as

$$\hat{G}(E,\mathbf{k}) \simeq \hat{P}(\mathbf{k})G(E,\mathbf{k}), \tag{21}$$

where

$$G(E,\mathbf{k}) = \frac{1}{E - E_{\mathbf{k}} - \Sigma}, \tag{22}$$

Σ is the disorder-induced self-energy and $\hat{P}$ is the upper-band projector given by

$$\hat{P}(\mathbf{k}) = |\chi_{\mathbf{k}}\rangle\langle\chi_{\mathbf{k}}|. \tag{23}$$

The spinors $|\chi_{\mathbf{k}}\rangle$ "dress" the matrix element of disorder by an angular-dependent factor $\langle\chi_{\mathbf{k}}|\chi'_{\mathbf{k}}\rangle$ [45]:

$$V_{\mathbf{k},\mathbf{k}'} \to \tilde{V}_{\mathbf{k},\mathbf{k}'} = V_{\mathbf{k},\mathbf{k}'}\langle\chi_{\mathbf{k}}|\chi'_{\mathbf{k}}\rangle.$$

Using Eq. (15) we find

$$\tilde{V}_{\mathbf{k}\mathbf{k}'} = V_{\mathbf{k}\mathbf{k}'}\langle\chi_{\mathbf{k}}|\chi'_{\mathbf{k}}\rangle = V_{\mathbf{k}\mathbf{k}'}\frac{1 + \eta\,\exp[i(\phi_{\mathbf{k}'} - \phi_{\mathbf{k}})]}{1+\eta}. \tag{24}$$

In other words, one can use a single-band approximation with the particles described by the Green's functions (22) with self-energy Σ determined by the spinor-dressed disorder (24).

The quantum scattering rate $\gamma = 1/\tau$ (the imaginary part of the self-energy) is related to the disorder correlation function (20) as follows:

$$\gamma = \int_0^{2\pi}\frac{d\phi}{2\pi}\gamma_D(\phi) = \gamma_W\frac{1+\eta^2}{(1+\eta)^2}, \tag{25}$$

where

$$\gamma_D(\phi_{\mathbf{k}}-\phi_{\mathbf{k}'}) = \frac{2\pi}{\hbar}\int \langle|\tilde{V}_{\mathbf{k}\mathbf{k}'}|^2\rangle\delta(E_{\mathbf{k}}-E_{\mathbf{k}'})\frac{k'dk'}{2\pi}$$
$$= \gamma_W\left|\frac{1+\eta e^{-i(\phi_{\mathbf{k}}-\phi_{\mathbf{k}'})}}{1+\eta}\right|^2$$
$$= \gamma_W\frac{1+2\eta\cos(\phi_{\mathbf{k}}-\phi_{\mathbf{k}'})+\eta^2}{(1+\eta)^2} \quad (26)$$

($\langle\ldots\rangle$ denotes the disorder averaging), and

$$\gamma_W = \frac{2\pi\nu_F}{\hbar}W. \quad (27)$$

Although we consider the short-range scattering potential, function $\gamma_D(\phi_{\mathbf{k}}-\phi_{\mathbf{k}'})$ turns out to be angle dependent due to the "dressing" by the factor $|\langle\chi_{\mathbf{k}}|\chi_{\mathbf{k}'}\rangle|^2$. As a consequence, the transport scattering rate

$$\gamma_{tr} = \int_0^{2\pi}\frac{d\phi}{2\pi}\gamma_D(\phi)(1-\cos\phi) = \gamma_W\frac{1+\eta^2-\eta}{(1+\eta)^2} \quad (28)$$

differs from the total (quantum) rate

$$\frac{\gamma}{\gamma_{tr}} = \frac{1+\eta^2}{1+\eta^2-\eta}. \quad (29)$$

It is well known (see Ref. [63] for detailed discussion) that the quantum conductivity corrections can be expressed in terms of the Cooperon propagator. Such a propagator obeys kinetic equation which can be derived by means of standard diagrammatic technique. The collision integral of this equation contains both ingoing and outgoing terms describing the scattering from the momentum $\mathbf{k}'$ to the momentum $\mathbf{k}$. The outgoing rate is determined by the rate $\gamma = \mathrm{Im}\Sigma$ entering the single-particle Green's function (22). To find the ingoing rate, we notice that the disorder vertex lines in the Cooperon propagator are also "dressed" by the Dirac spinor factors. The two-particle amplitude of the scattering from $\mathbf{k}'$ to $\mathbf{k}$ is dressed by $\langle\chi_{\mathbf{k}}|\chi_{\mathbf{k}'}\rangle\langle\chi_{-\mathbf{k}}|\chi_{-\mathbf{k}'}\rangle$ (here we neglected the momentum transferred through disorder vertex lines in these factors). Hence, the ingoing rate $\gamma_C(\phi_{\mathbf{k}}-\phi_{\mathbf{k}'})$ is given by Eq. (26) with the replacement $\langle|\tilde{V}_{\mathbf{k}\mathbf{k}'}|^2\rangle$ with $\langle\tilde{V}_{\mathbf{k}\mathbf{k}'}\tilde{V}^*_{-\mathbf{k}',-\mathbf{k}}\rangle$. Simple calculation yields (here and below, for the sake of brevity we replace $\phi_{\mathbf{k}}\to\phi$ and $\phi'_{\mathbf{k}}\to\phi'$)

$$\gamma_C(\phi-\phi') = \gamma_W\left[\frac{1+\eta e^{-i(\phi-\phi')}}{1+\eta}\right]^2 = \sum_M \gamma_M e^{iM(\phi-\phi')}, \quad (30)$$

where

$$\gamma_0 = \frac{\gamma}{1+\eta^2}, \quad \gamma_{-1} = \frac{2\eta\gamma}{1+\eta^2}, \quad \gamma_{-2} = \frac{\eta^2\gamma}{1+\eta^2}, \quad (31)$$

and $\gamma_M = 0$ for $M\neq 0,-1,-2$. We see that the outgoing rate considered as a function of ϕ contains only three harmonics: $M = 0,-1,-2$. Remarkably,

$$\gamma_M \neq \gamma, \quad \text{for any } M, \quad (32)$$

that means that the Cooperon propagator has a finite decay rate even in the absence of the inelastic scattering [43]. More specifically, the kernel of the collision integral can be written as

$$\gamma_C(\phi-\phi')-\gamma\delta(\phi-\phi')$$
$$= -\frac{\gamma}{1+\eta^2}[\eta^2+(1-\eta)^2e^{-i(\phi-\phi')}+e^{-2i(\phi-\phi')}]$$
$$-\gamma\sum_{M\neq 0,-1,-2}e^{iM(\phi-\phi')}.$$

We see that in the limit $\eta\to 0$ (orthogonal class), the Cooperon mode with the moment $M=0$ does not decay, while for $\eta\to 1$ (symplectic class) there is also a nondecaying mode with the moment $M=-1$. However, for arbitrary η all modes decay. We also note that the function $\gamma_C(\phi)$ is asymmetric with respect to inversion of the scattering angle $\phi\to-\phi$:

$$\gamma_C(\phi) = \gamma_C^*(-\phi) \neq \gamma_C(-\phi). \quad (33)$$

Equation (30) for the ingoing scattering rate in the Cooper channel was derived for the block II. One can easily show that in the block I the ingoing rate is given by the equation which is complex conjugated to Eq. (30): $\gamma_C(\phi)\to\gamma_C^*(\phi)$.

In the end of this section, we note that for $\eta=0$ the system is in the orthogonal symmetry class (the two-particle scattering amplitude has no angular dependence), whereas the limit $\eta=1$ corresponds to the symplectic symmetry class with the disorder scattering dressed by the "Berry phase." The intermediate case corresponds to the unitary symmetry class, where the quantum interference is partially killed by the Berry-phase fluctuations (see discussion in Sec. IV C).

III. KINETIC EQUATION FOR THE COOPERON

With the projection on the upper band and dressing the disorder correlation functions in the Cooperon ladders, the calculation of the correction to the conductivity reduces to the solution of a kinetic equation for a Cooperon propagator moving in an effective disorder characterized by the correlation functions (30) in the ingoing part of the collision integral and by (26) in the outgoing term. This equation is analyzed below separately for the cases of zero and nonzero magnetic fields. In this section, we focus on the contribution of the block II. Contribution of the block I will be discussed in Sec. IV B.

A. Zero magnetic field

The kinetic equation for the Cooperon in $(\mathbf{q},\omega)$ domain at $\omega=0$ has the form

$$[1/\tau_\phi + i\mathbf{q}\mathbf{v}_F]C_{\mathbf{q}}(\phi,\phi_0)$$
$$= \int\frac{d\phi'}{2\pi}[\gamma_C(\phi-\phi')C_{\mathbf{q}}(\phi',\phi_0)-\gamma_D(\phi-\phi')C_{\mathbf{q}}(\phi,\phi_0)]$$
$$+\gamma\delta(\phi-\phi_0). \quad (34)$$

Introducing dimensionless variables

$$\Gamma = 1/\gamma\tau_\phi, \quad \mathbf{Q} = \mathbf{q}l, \quad (35)$$

where

$$l = \frac{v_F}{\gamma} = \frac{2\hbar^3 v}{mW_0}\frac{\sqrt{\eta}(1-\eta)}{1+\eta^2} \quad (36)$$

is the mean-free path, we rewrite Eq. (34) as follows:

$$(1+\Gamma+i\mathbf{Qn})C_{\mathbf{Q}}(\phi,\phi_0) = \int \frac{d\phi'}{2\pi}\frac{[1+\eta e^{-i(\phi-\phi')}]^2}{1+\eta^2}C_{\mathbf{Q}}(\phi',\phi_0)+\delta(\phi-\phi_0), \quad (37)$$

where $\mathbf{n}=(\cos\phi,\sin\phi)$.

Before solving this equation, we note that the Fourier transform of the Cooperon propagator gives (see Ref. [63]) the quasiprobability (per unit area) for electron starting with momentum direction $\mathbf{n}_0$ from initial point $\mathbf{r}_0$ to arrive at the point $\mathbf{r}$ with the momentum direction $\mathbf{n}$:

$$C(\phi,\phi_0,\mathbf{r}-\mathbf{r}_0)=\frac{1}{l^2}\int\frac{d^2\mathbf{Q}}{(2\pi)^2}e^{i\mathbf{Q}(\mathbf{r}-\mathbf{r}_0)/l}C_{\mathbf{Q}}(\phi,\phi_0). \quad (38)$$

In particular, the conductivity can be expressed in terms of this "probability" taken at $\mathbf{r}-\mathbf{r}_0=0$, so-called "return probability" [63]

$$W(\phi-\phi_0)=C(\phi,\phi_0,0). \quad (39)$$

It is worth noting that return "probability" which was defined above as a formal solution of the kinetic equation for the Cooperon can be negative or complex.

Usually, the solution of the Cooperon kinetic equation is searched in the diffusion approximation. Within such an approximation, one can obtain a solution for an arbitrary type of the disorder. It is also known that in the case of the short-range disorder, when the collision integral contains only zero harmonic with the moment 0, the exact solution can be found which is valid beyond the diffusion approximation and, consequently, describes the ballistic case. As seen from Eq. (37), in our case the incoming term of the collision integral contains only three angular harmonics with the moments $0,-1$, and -2. This allows one to find the exact solution of Eq. (37) valid beyond the diffusion approximation. The details of the calculations are presented in Appendix A 1. We find that the return probability is given by

$$W(\phi)=\frac{1}{2\pi l^2}\sum_{n=-\infty}^{\infty}w_n e^{i(n-1)\phi}, \quad (40)$$

where

$$w_n=\int\frac{d^2\mathbf{Q}}{(2\pi)^2}\begin{bmatrix}P_{n-1}\\P_n\\P_{n+1}\end{bmatrix}^T\left(\hat{M}^{-1}-\hat{M}^{-1}_{Q=\infty}\right)\begin{bmatrix}P_{n-1}\\P_n\\P_{n+1}\end{bmatrix}, \quad (41)$$

and matrix $\hat{M}$ reads as

$$\hat{M}=\begin{bmatrix}1+\eta^2-P_0 & -P_1 & -P_2\\ -P_1 & \frac{1+\eta^2}{2\eta}-P_0 & -P_1\\ -P_2 & -P_1 & \frac{1+\eta^2}{\eta^2}-P_0\end{bmatrix}. \quad (42)$$

Here,

$$P_n=\int\frac{d\phi}{2\pi}\frac{e^{-in\phi}}{1+\Gamma+iQ\cos\phi} \quad (43)$$

$$=(-i)^{|n|}P_0\left[\frac{1-P_0(1+\Gamma)}{1+P_0(1+\Gamma)}\right]^{|n|/2} \quad (44)$$

and

$$P_0=\frac{1}{\sqrt{(1+\Gamma)^2+Q^2}}. \quad (45)$$

On the technical level, the logarithmic divergency of conductivity, specific for WL (WAL) corrections, comes from singular behavior of the matrix $\hat{M}^{-1}$ at $Q\to 0$. Let us consider the limiting case $Q=0$, $\Gamma=0$. In this case $P_0=1$, $P_1=P_2=0$, and we find

$$\hat{M}^{-1}=\begin{pmatrix}\frac{1}{\eta^2} & 0 & 0\\ 0 & \frac{2\eta}{(1-\eta)^2} & 0\\ 0 & 0 & \eta^2\end{pmatrix}. \quad (46)$$

Then, in the limit $\eta\to 0$ (orthogonal class), the singular mode corresponds to $M=0$ [see Eq. (A1)] and $C_{\mathbf{Q}=0}(\phi,\phi_0)\propto 1/\eta^2$, while in the limit $\eta\to 1$ (symplectic class) the singular mode corresponds to $M=-1$ and $C_{\mathbf{Q}=0}(\phi,\phi_0)\propto e^{-i(\phi-\phi_0)}/(1-\eta)^2$.

B. Nonzero magnetic field

Now, we assume that the magnetic field B is applied to the system perpendicular to the plane of the well. For sufficiently weak fields when the mean-free path is smaller than the cyclotron radius, the bending of the trajectories by the magnetic field can be neglected, and the only effect of the field is the phase difference between two trajectories propagating along a closed loop in the opposite directions. This phase can be taken into account by rewriting Eq. (34) in the $(\omega,\mathbf{r})$ representation and modification of the operator $\mathbf{q}$ as follows: $\hat{\mathbf{q}}=-i\partial/\partial\mathbf{r}+2e\mathbf{A}/c\hbar$, where $\mathbf{A}=(By,0)$ is the vector potential in the Landau gauge. The components of this operator

$$\hat{q}_x=-i\frac{\partial}{\partial x}+\frac{y}{l_B^2},\quad \hat{q}_y=-i\frac{\partial}{\partial y} \quad (47)$$

obey the following commutation rule:

$$[\hat{q}_x,\hat{q}_y]=\frac{i}{l_B^2}\mathrm{sign}(B). \quad (48)$$

Here,

$$l_B=\sqrt{\frac{\hbar c}{2e|B|}} \quad (49)$$

is the magnetic length for the particle with the charge $2e$.

Instead of Eq. (37), we get

$$[1+\Gamma+il\hat{\mathbf{q}}\mathbf{n}]C(\mathbf{r},\mathbf{r}_0,\phi,\phi_0) = \int\frac{d\phi'}{2\pi}\frac{[1+\eta e^{-i(\phi-\phi')}]^2}{1+\eta^2}C(\mathbf{r},\mathbf{r}_0,\phi',\phi_0) + \delta(\mathbf{r}-\mathbf{r}_0)\delta(\phi-\phi_0), \quad (50)$$

where $\hat{\mathbf{q}}\mathbf{n}=\hat{q}_x\cos\phi+\hat{q}_y\sin\phi$ and $\hat{q}_x,\hat{q}_y$ are given by Eq. (47). Exact solution of this equation valid beyond the diffusion approximation is obtained in Appendix A 2. We demonstrate that return probability is given by Eq. (40) where

w_n are now given by

$$w_n = \frac{l^2}{2\pi l_B^2}\sum_{m=-\infty}^{\infty}\begin{bmatrix}P_{n+m,m+1}\\ P_{n+m,m}\\ P_{n+m,m-1}\end{bmatrix}^T\left(\hat{M}_m^{-1}-\hat{M}_{m=\infty}^{-1}\right)\begin{bmatrix}P_{n+m,m+1}\\ P_{n+m,m}\\ P_{n+m,m-1}\end{bmatrix}. \tag{51}$$

Here,

$$\hat{M}_m = \begin{bmatrix}1+\eta^2-P_{m+1,m+1} & -P_{m+1,m} & -P_{m+1,m-1}\\ -P_{m+1,m} & \frac{1+\eta^2}{2\eta}-P_{m,m} & -P_{m,m-1}\\ -P_{m+1,m-1} & -P_{m,m-1} & \frac{1+\eta^2}{\eta^2}-P_{m-1,m-1}\end{bmatrix} \tag{52}$$

and

$$P_{nm} = \frac{l_B}{l}\left[\frac{\min(n,m)!}{\max(n,m)!}\right]^{1/2}\theta(n)\theta(m)\int_0^\infty dt\, e^{-t(1+\Gamma)l_B/l}e^{-t^2/4}\left(\frac{-it}{\sqrt{2}}\right)^{|n-m|}L_{\min(n,m)}^{|n-m|}\left(\frac{t^2}{2}\right), \tag{53}$$

where L_N^k are generalized Laguerre polynomials. Although P_{nm} are defined for $n \geq 0$ and $m \geq 0$, it is convenient to introduce theta functions $\theta(n)$ and $\theta(m)$ [$\theta(n) = 1$ for $n \geqslant 0$ and $\theta(n) = 0$ for $n < 0$] in the definition of P_{nm}, assuming that they are defined for arbitrary integers n and m. From Eq. (53) we see that $P_{nm} = P_{mn}$. One can check that w_n are real, in spite of the fact that P_{nm} contains factor $i^{|n-m|}$.

Let us now demonstrate that for $B \to 0$, Eq. (51) coincides with Eq. (41). Using the asymptotical Tricomi expression for generalized Laguerre polynomials

$$L_n^\alpha(t^2) \approx \frac{e^{t^2/2}}{t^\alpha}\left(n+\frac{\alpha+1}{2}\right)^{\alpha/2} \times J_\alpha\left(2\sqrt{n+\frac{\alpha+1}{2}}t\right) \quad \text{for } n\to\infty$$

(here J_α is the Bessel function), we find from Eq. (53)

$$P_{m,m+\alpha} \to P_\alpha(Q_{m,\alpha}) \quad \text{for } m\to\infty, \tag{54}$$

where

$$Q_{m,\alpha} = \frac{l}{l_B}\sqrt{2m+\alpha+1} \tag{55}$$

and $P_\alpha(Q)$ is given by Eq. (43). Substituting Eq. (54) into Eqs. (52) and (51), neglecting at large m dependence of $Q_{m,\alpha}$ on α, and replacing summation over m in Eq. (51) with integration over $dQ^2 l_B^2/2l^2$, after simple calculations we arrive to Eq. (41).

Finally, we note that Eqs. (51) and (52) were derived for block II. Analogous equations valid in the block I are presented in Sec. IV B.

C. Diffusion approximation

The diffusion approximation is valid provided that the typical length of interfering diffusive trajectory is long compared to the mean-free path l. On the formal level, this implies that there is a diffusive Cooperon mode with the gap much smaller than γ. To guarantee that this condition is fulfilled, we assume that $\Gamma \ll 1$, dimensionless magnetic field

$$b = \frac{l^2}{2l_B^2}\text{sign(B)} \tag{56}$$

is weak, $|b| \ll 1$, and one of the conditions $\eta \ll 1$ or $1-\eta \ll 1$ is satisfied. In this case, calculation of w_n essentially simplifies. Let us start with discussion of the case of zero field and then generalize obtained results for the case of finite fields.

(a) $b = 0$. The formal solution of Eq. (34) is written as

$$\hat{C} = \frac{\gamma}{\gamma+\gamma_\varphi-\hat{\gamma}_C+i\mathbf{qn}}, \tag{57}$$

where $\gamma_\varphi = 1/\tau_\varphi$ and the kernel of the operator $\hat{\gamma}_C$ is given by Eq. (30). For $ql \ll 1$, we find from Eq. (57)

$$C_{\mathbf{q}}(\phi,\phi_0) \approx \frac{\gamma}{2\pi}\sum_M \frac{e^{iM(\phi-\phi_0)}}{\tau_M^{-1}+v_F^2\left\langle \mathbf{qn}\frac{1}{\gamma+\gamma_\varphi-\hat{\gamma}_C}\mathbf{qn}\right\rangle_M} = \frac{\gamma}{2\pi}\sum_M \frac{e^{iM(\phi-\phi_0)}}{\tau_M^{-1}+q^2D_M},$$

where

$$\tau_M = \frac{1}{\gamma_\varphi+\gamma-\gamma_M}, \tag{58}$$

$$D_M = \frac{v_F^2(\tau_{M+1}+\tau_{M-1})}{4}, \tag{59}$$

$\langle\ldots\rangle_M$ stands for projection on the Mth harmonic and γ_M are given by Eq. (31) We note that for calculation D_M one may set $\gamma_\varphi = 0$ in Eq. (58). Within this approximation, we find $\tau_0 = (1+\eta^2)/\gamma\eta^2, \tau_{-1} = (1+\eta^2)/\gamma(1-\eta)^2, \tau_{-2} = (1+\eta^2)/\gamma$, and $\tau_M = 1/\gamma$, for $M \neq 0,-1,-2$. Here, we took into account that $\Gamma \ll 1 (\gamma_\varphi \ll \gamma)$. For w_M, we find

$$w_M = \int_{ql\lesssim 1}\frac{l^2d^2\mathbf{q}}{(2\pi)^2}\frac{\gamma}{\tau_{M-1}^{-1}+q^2D_{M-1}}. \tag{60}$$

Since we use the diffusion approximation, the integration in Eq. (60) is limited by small $q: ql \lesssim 1$.

(b) $b \neq 0$. In this case, one should take into account that operators $\hat{q}_x$ and $\hat{q}_y$ no longer commute [see Eq. (48)]. Simple calculation yields

$$v_F^2\left\langle \hat{\mathbf{qn}}\frac{1}{\gamma+\gamma_\varphi-\hat{\gamma}_C}\hat{\mathbf{qn}}\right\rangle_M = \left(\hat{q}_x^2+\hat{q}_y^2\right)D_M + i[\hat{q}_x,\hat{q}_y]\tilde{D}_M, \tag{61}$$

where

$$\tilde{D}_M = \frac{v_F^2(\tau_{M-1} - \tau_{M+1})}{4}. \tag{62}$$

As a next step, one should replace in Eq. (61) the operator $\hat{q}_x^2 + \hat{q}_y^2$ by its eigenvalue $\hat{q}_x^2 + \hat{q}_y^2 = (4/l^2)|b|(n + 1/2)$. Importantly, the operator $\hat{q}_x^2 + \hat{q}_y^2$ is positively defined and depends on the absolute value of the magnetic field. In contrast, commutator $[\hat{q}_x, \hat{q}_y]$ changes sign with inversion of field. Hence, Eq. (61) contains the sum of two equations of different parity with respect to the field inversion:

$$v_F^2 \left\langle \hat{\mathbf{q}}\mathbf{n} \frac{1}{\gamma + \gamma_\varphi - \hat{\gamma}_C} \hat{\mathbf{q}}\mathbf{n} \right\rangle_M = \frac{2}{l^2}[|b|(2n+1)D_M - b\tilde{D}_M]. \tag{63}$$

One should also modify Eq. (60) by replacing the integral over $d^2\mathbf{q}$ with the sum over n:

$$\int_{ql<1} \frac{l^2 d^2\mathbf{q}}{(2\pi)^2} \to \frac{|b|}{\pi} \sum_{n=0}^{N}, \tag{64}$$

where $N \propto 1/|b|$ limits the region where diffusion approximation is applicable. Analytical expression for w_M reads as

$$w_M = \frac{|b|}{\pi} \sum_{n=0}^{N} \frac{\gamma l^2}{l^2/\tau_{M-1} + 2|b|(2n+1)D_{M-1} - 2b\tilde{D}_{M-1}}. \tag{65}$$

We see that w_M turns out to be asymmetric with respect to inversion of b: $w_M(b) \neq w_M(-b)$, so that contribution to the conductivity correction coming from a single cone is an asymmetric function of b. Of course, after summing contributions of two cones, conductivity becomes an even function of magnetic field as it should be.

IV. INTERFERENCE CORRECTION TO THE CONDUCTIVITY

A. Contribution of the single Dirac cone

In this section, we calculate the contribution to the interference correction coming from the single cone. We will use expressions derived in the previous section for the Cooperon propagator in the block II.

The Cooperon propagator enters as a building block into diagrams describing the quantum correction to the conductivity. Such diagrams can be calculated in a standard way. However, instead of formal summation of the diagrams, one can use a semiclassical method developed in Ref. [60]. It was shown in this paper that there are two contributions to the coherent scattering, so-called backscattering and nonbackscattering contributions. Both of them can be expressed in terms of renormalization of the cross section of the scattering by a single impurity. The main advantage of this method compared to the standard diagrammatic machinery is the simplicity of the calculations and the physical transparency that will allow us to clarify the physical sense of the obtained results. This method is based on considering the trajectories corresponding to the condition of the phase stationarity. Such trajectories give the dominant contribution in the weak localization regime, when $k_F l \gg 1$. The method was developed in Ref. [60] for the case of the isotropic scattering of spinless particle by a short-range potential, that corresponds to $\eta \to 0$ in our notations. Generalization for the case of finite η is straightforward. The only additional ingredient of the discussed problem is the spin projectors [Eq. (23)] entering Green's functions [Eq. (21)]. As we already mentioned above, such projectors can be taken into account by dressing of the disorder correlation functions. Following, we demonstrate it by discussing the simplest coherent scattering processes at a scattering complex consisting of $N = 5$ impurities. Such processes and corresponding diagrams are shown in Figs. 1 and 2.

The coherent backscattering process plotted in Fig. 1(a) corresponds to diagram shown in Fig. 1(c). In this process, two electron waves with the amplitude A (solid line) and B (dashed line) start at the point i and interfere at the point f after traveling in the opposite directions around a closed loop formed by impurities $1,2,\ldots,N$. The contribution of this process to the conductivity is proportional to AB^*. This process leads to correction to the scattering cross section (delta peaked at the scattering angle $\phi = \pi$) of the impurity 1 (for a more detailed discussion, see Ref. [60]). The scatterings on impurities $2,3,\ldots,N$ are dressed by spinor factors and described by the Cooperon correlation function γ_C defined by Eq. (30). One can easily show that the impurity 1 is also dressed by a spinor factor proportional to $\gamma_C(\pi - \phi)$, where ϕ is the angle between $\mathbf{n}$ and $\mathbf{n}_0$ [see Fig. 1(a)]. The process shown in Fig. 1(b) leads to nonbackscattering contribution described by diagram shown in Fig. 1(d). One can easily check that in this process the impurity 1 is dressed by the same spinor factor $\propto\gamma_C(\pi - \phi)$. The sum of these two processes and the processes Figs. 2(a) and 2(b) [described by diagrams 2(c) and 2(d), respectively] which are complex conjugated to Figs. 1(c) and 1(d) leads to the correction to the scattering cross section:

$$\frac{\delta\Sigma(\phi)}{\Sigma_{tr}} \approx \lambda_F l_{tr} \frac{1}{\gamma} \left[\delta(\phi - \pi) \int d\phi' \gamma_C(\pi - \phi') W(\phi') - \gamma_C(\pi - \phi) W(\phi) \right],$$

where first and second terms represent backscattering and nonbackscattering contributions, respectively. Here, $\lambda_F l_{tr}$ is the effective return area and the coefficient $1/\gamma$ appeared due to the normalization of the Cooperon propagator [see coefficient γ in front of the delta function in Eq. (34)]. The quantum correction to the cross section incorporating both types of the coherent processes is given by $\int (d\phi/2\pi)\delta\Sigma(\phi)(1 - \cos\phi)$ and corresponding conductivity correction reads as

$$\delta\sigma_{\rm II} = -\frac{e^2}{\hbar} \left(\frac{l_{tr}}{l}\right)^2 l^2 \int \frac{d\phi}{2\pi} \frac{\gamma_C(\pi - \phi)}{\gamma} W(\phi)(1 + \cos\phi). \tag{66}$$

Equation (66) can be also derived within the standard diagrammatic approach, in which factor l^2 appears due to the integration over coordinates of the points i and f, whereas factor $(l_{tr}/l)^2$ accounts for the transportization of the vertexes.

As a result, we obtain

$$\delta\sigma_{\rm II} = -\frac{e^2}{\hbar}\frac{(1+\eta^2)l^2}{(1+\eta^2-\eta)^2} \times \int \frac{d\phi}{2\pi}(1-2\eta e^{i\phi}+\eta^2 e^{2i\phi})W(\phi)(1+\cos\phi), \tag{67}$$

or, finally, with the use of Eq. (40)

$$\delta\sigma_{\rm II} = -\frac{e^2}{2\pi\hbar}\frac{1+\eta^2}{(1+\eta^2-\eta)^2}\left[(1-\eta)w_1+\frac{1+\eta^2-4\eta}{2}w_0 + \frac{w_2}{2}+(\eta^2-\eta)w_{-1}+\frac{\eta^2}{2}w_{-2}\right], \tag{68}$$

where w_n are given by Eqs. (41) and (51) for $B=0$ and $B\neq 0$, respectively.

As we mentioned above, for $\eta\to 0$ and 1 one of the modes becomes singular and diffusion approximation is applicable provided that $\Gamma \ll 1$, $|b|\ll 1$. Next, we consider limiting cases described within this approximation. One can use two alternative approaches: to explore simplified equations obtained in Sec. III C or obtain results directly from rigorous equations (41) and (51). In the following two subsections, we use the first approach. In Appendix B, we demonstrate that the second approach yields the same results.

At the end of this section, we note that the conductivity correction, Eq. (68), is invariant over the replacement $\eta\to 1/\eta$. As was explained in Sec. II A, this means that although this equation was derived for the normal case, it equally applies for inverted semiconductor both for the electron and the hole spectrum branches.

1. Limiting cases for $B=0$

(a) $\eta\to 0$. As seen from Eq. (60), in this case the singular contribution comes from w_1 because $\tau_0^{-1}=\gamma_\varphi+\gamma\eta^2/(1+\eta^2)\to\gamma_\varphi+\gamma\eta^2\ll\gamma$. The diffusion coefficient entering Eq. (60) reads as $D_0\approx v_F^2/2\gamma$, so that from Eqs. (60) and (68) we find

$$\delta\sigma_{\rm II}\approx -\frac{e^2}{4\pi^2\hbar}\ln\left(\frac{1}{\eta^2+\Gamma}\right). \tag{69}$$

(b) $\eta\to 1$. The singular contribution comes from w_0 because $\tau_{-1}^{-1}\to\gamma_\varphi+\gamma(1-\eta)^2/2\ll 1$. The diffusion coefficient in this mode reads as $D_{-1}\approx v_F^2/\gamma$. From Eqs. (60) and (68), we obtain

$$\delta\sigma_{\rm II}\approx \frac{e^2}{4\pi^2\hbar}\ln\left[\frac{1}{(1-\eta)^2/2+\Gamma}\right]. \tag{70}$$

A more general approach based on exact equation (41) allows one to find analytically corrections to Eqs. (69) and (70) [45]:

$$\delta\sigma_{\rm II}\approx\frac{e^2}{4\pi^2\hbar}\begin{cases}-\left(1-\frac{5\eta^2}{2}\right)\ln\left(\frac{1}{\eta^2}\right)+\ln 2+4\eta\ln 2-\eta+O(\eta^2) & \text{for}\quad \eta\to 0,\\ \left[1-\frac{7(1-\eta)^2}{2}\right]\ln\left[\frac{1}{(1-\eta)^2}\right]+3(\ln 2-1)+\eta-1+O[(1-\eta)^2] & \text{for}\quad \eta\to 1.\end{cases} \tag{71}$$

For simplicity, we neglected here dephasing processes thus setting $\Gamma=0$. [For comparison of Eq. (71) in the limit $\eta\to 1$ with the previously obtained results [43], see Ref. [45].]

2. Limiting cases for $B\neq 0$

(a) $\eta\to 0$. In this case, $\tilde{D}_0\approx\eta v_F^2/2\gamma$ and from Eq. (65) we find the expression for the singular mode

$$w_1=\frac{|b|}{\pi}\sum_{n=0}^{N}\frac{1}{\Gamma+\eta^2+2|b|(n+1/2)-b\eta}. \tag{72}$$

Let us introduce the function

$$h(|b|,A)=\sum_{n=0}^{N\sim 1/|b|}\frac{|b|}{|b|(n+1/2)+A} \approx \ln\left(\frac{C_*}{|b|}\right)-\psi(A/|b|+1/2), \tag{73}$$

where

$$\psi(z)=\sum_{k=1}^{\infty}\left(\frac{1}{k}-\frac{1}{k+z-1}\right)-C$$

is the digamma function, C is the Euler constant, and the field-independent coefficient $C_*\sim N|b|\sim 1$ is determined by the ballistic effects and can not be found within the diffusion approximation. We will see that this coefficient drops out from the equation for the magnetoconductivity [see Eq. (77)]. Asymptotical behavior of $h(|b|,A)$ in the limits of weak and strong fields can be found with the use of the following asymptotic of $\psi(z)$:

$$\psi(z)\approx\ln z-\frac{1}{2z}-\frac{1}{12z^2}\quad\text{for}\quad z\gg 1. \tag{74}$$

In our case, $A=(\Gamma+\eta^2-b\eta)/2$ and the variable $z=b_*/|b|+1/2-\eta b/2|b|$ changes in the following interval: $(1-\eta)/2<z<\infty$. Here,

$$b_*=\frac{\Gamma+\eta^2}{2}.$$

From Eqs. (73) and (74), we find

$$h\left(|b|,\frac{\Gamma+\eta^2-b\eta}{2}\right)\approx\begin{cases}\ln\left(\frac{C_*}{b_*}\right)+\frac{\eta b}{2b_*}-\frac{b^2}{24b_*^2} & \text{for}\quad |b|\ll b_*,\\ \ln\left(\frac{C_*}{|b|}\right)-\psi(1/2)-\frac{\pi^2}{2}\frac{b_*-\eta b/2}{|b|} & \text{for}\quad b_*\ll|b|\ll 1.\end{cases}\tag{75}$$

We see that function h is asymmetric with respect to inversion of the magnetic field. In the low-field limit, the asymmetry is due to the term $\eta b/2b_*$, which shifts the position of the maximum of h from point $b=0$ to the point $b=6\eta b_*$. In the opposite strong-field limit, a small asymmetry comes from the term $\pi^2 b/4|b|$, which arises as a result of expansion of the digamma function near the point $z=\frac{1}{2}$ [in order to avoid cumbersome equations, in the following we neglect everywhere small correction $-\psi(1/2)-(\pi^2/2)(b_*-\eta b/2)/|b|$ to the logarithmic strong-field asymptotic of h].

The function w_1 is expressed in terms of function h as follows:

$$w_1=h\left(|b|,\frac{\Gamma+\eta^2-b\eta}{2}\right)\Big/2\pi.\tag{76}$$

Using Eqs. (68), (75), and (76) we find

$$\begin{aligned}\Delta\sigma_{\rm II}&=\delta\sigma_{\rm II}(b)-\delta\sigma_{\rm II}(0)\\&=-\frac{e^2}{4\pi^2\hbar}\left[h\left(|b|,\frac{\Gamma+\eta^2-b\eta}{2}\right)-h\left(0,\frac{\Gamma+\eta^2}{2}\right)\right]\\&\approx-\frac{e^2}{4\pi^2\hbar}\begin{cases}\frac{\eta b}{2b_*}-\frac{b^2}{24b_*^2} & \text{for}\quad |b|\ll b_*,\\ \ln\left(\frac{b_*}{|b|}\right) & \text{for}\quad |b|\gg b_*.\end{cases}\end{aligned}\tag{77}$$

Remarkably, Eq. (77) contains the linear-in-b term in the limit of low fields. It is worth noting that this term can be taken into account on the formal level as renormalization of the Cooperon decay rate $\eta^2\to\eta^2-\eta b$ in the argument of the function h. The existence of linear contribution to the conductivity means that in a single Dirac cone the minimum of the conductivity correction as a function of b is shifted from the point $b=0$ to the point $b=6\eta b_*$. However, as we already mentioned, after summing contributions of two blocks, the linear-in-b terms existing in these blocks cancel each other.

(b) $\eta\to 1$. In this case, $\tilde{D}_{-1}\approx-(1-\eta)v_F^2/\gamma$ and from Eq. (65) we find

$$w_0=\frac{|b|}{\pi}\sum_{n=0}^{N}\frac{1}{\Gamma+(1-\eta)^2/2+2|b|(2n+1)+2b(1-\eta)}.\tag{78}$$

By using the asymptotic of the digamma function, we find for the conductivity correction

$$\begin{aligned}\Delta\sigma_{\rm II}&=\delta\sigma_{\rm II}(b)-\delta\sigma_{\rm II}(0)\\&=\frac{e^2}{4\pi^2\hbar}\left\{h\left[|b|,\frac{\Gamma+(1-\eta)^2/2+2b(1-\eta)}{4}\right]-h\left[0,\frac{\Gamma+(1-\eta)^2/2}{4}\right]\right\}\\&\approx\frac{e^2}{4\pi^2\hbar}\begin{cases}-\frac{(1-\eta)b}{2b_*}-\frac{b^2}{24b_*^2} & \text{for}\quad |b|\ll b_*,\\ \ln\left(\frac{b_*}{|b|}\right) & \text{for}\quad b_*\ll|b|\ll 1,\end{cases}\end{aligned}\tag{79}$$

where

$$b_*=\frac{\Gamma+(1-\eta)^2/2}{4}.$$

Again, we see that Eq. (79) contains the linear-in-b term in the limit of low fields. We also see that this term can be formally taken into account by renormalization of the Cooperon decay rate $(1-\eta)^2/2\to(1-\eta)^2/2+2(1-\eta)b$ in the argument of the function h.

B. Contribution of the other Dirac cone and inversion of the sign of the magnetic field

Next, we take into account the contribution to the conductivity correction coming from the block I. The only difference is that the scattering rate $\gamma_C(\phi-\phi')$ is given by the equation which is complex conjugated to Eq. (30):

$$\gamma_C(\phi-\phi')=\gamma_W\left[\frac{1+\eta e^{i(\phi-\phi')}}{1+\eta}\right]^2.\tag{80}$$

The calculations are quite analogous to the ones presented above. The return probability reads as

$$W(\phi)=\frac{1}{2\pi l^2}\sum_{n=-\infty}^{\infty}w_n e^{-i(n-1)\phi}\tag{81}$$

[we notice sign minus in the exponent compared to Eq. (40)], where

$$w_n=\frac{l^2}{2\pi l_B^2}\sum_{m=-\infty}^{\infty}\begin{bmatrix}P_{m-n,m-1}\\P_{m-n,m}\\P_{m-n,m+1}\end{bmatrix}^T\left(\hat{M}_m^{-1}-\hat{M}_{m=\infty}^{-1}\right)\begin{bmatrix}P_{m-n,m-1}\\P_{m-n,m}\\P_{m-n,m+1}\end{bmatrix}\tag{82}$$

and

$$\hat{M}_m = \begin{bmatrix} 1+\eta^2 - P_{m-1,m-1} & -P_{m,m-1} & -P_{m+1,m-1} \\ -P_{m,m-1} & \frac{1+\eta^2}{2\eta} - P_{m,m} & -P_{m+1,m} \\ -P_{m+1,m-1} & -P_{m+1,m} & \frac{1+\eta^2}{\eta^2} - P_{m+1,m+1} \end{bmatrix}. \quad (83)$$

The contribution to the conductivity correction is expressed in terms of w_n according to Eq. (68). For zero field, Eq. (82) transforms to Eq. (41), so that the account for the second cone doubles the conductivity correction:

$$\delta\sigma_{\rm tot} = 2\delta\sigma_{\rm II}. \quad (84)$$

However, this is not the case for the nonzero field when the total conductivity correction is given by

$$\delta\sigma_{\rm tot} = \delta\sigma_{\rm I} + \delta\sigma_{\rm II}, \quad (85)$$

where $\delta\sigma_{\rm I}$ and $\delta\sigma_{\rm II}$ are found from Eqs. (82), (83), (53), (68) and Eqs. (51), (52), (53), and (68), respectively.

Let us now discuss what happens with the inversion of the sign of the magnetic field. Such inversion changes the sign of the commutator (48). The calculations fully analogous to those presented in Sec. III B and Appendix A 2 yield that the magnetic field inversion is equivalent to the replacement of $\delta\sigma_{\rm I}$ and $\delta\sigma_{\rm II}$:

$$\delta\sigma_{\rm I}(b) = \delta\sigma_{\rm II}(-b). \quad (86)$$

Importantly, $\delta\sigma_{\rm I}(b) \neq \delta\sigma_{\rm II}(b)$, $\delta\sigma_{\rm I}(b) \neq \delta\sigma_{\rm I}(-b)$, and $\delta\sigma_{\rm II}(b) \neq \delta\sigma_{\rm II}(-b)$. As we demonstrate in the following (see Sec. VI), numerical evaluation of the conductivity correction shows strong magnetic field asymmetry of the functions $\delta\sigma_{\rm I}(b)$ and $\delta\sigma_{\rm II}(b)$. Only the total conductivity correction is an even function of the magnetic field

$$\delta\sigma_{\rm tot}(b) = \delta\sigma_{\rm tot}(-b). \quad (87)$$

C. Interpretation of the obtained results in terms of the Berry phase

In this section, we will use the Berry-phase picture for a qualitative interpretation of the obtained results. We will follow the approach discussed in Ref. [52] in connection with the weak localization of holes and later on used for description of the interference corrections in the 2D HgTe/CdTe based TI [46] and topological crystalline insulators with a quadratic surface spectrum [47].

The Berry "vector potential" $\boldsymbol{\mathcal{A}}$ is defined as (see Refs. [46,52] and references therein)

$$\boldsymbol{\mathcal{A}} = i\langle\chi_{\mathbf{k}}|\frac{\partial}{\partial\mathbf{k}}|\chi_{\mathbf{k}}\rangle. \quad (88)$$

The Berry phase is given by the integration of the vector potential along a closed loop on the Fermi surface: $\Gamma_B = \oint \boldsymbol{\mathcal{A}} d\mathbf{k}$. Substituting into Eq. (88) spinor functions $\chi_{\mathbf{k}}^{(\rm I,+)}$ and $\chi_{\mathbf{k}}^{(\rm II,+)}$ we find after simple algebra

$$\Gamma_B^{\rm I} = -\Gamma_B^{\rm II} = \frac{2\pi\eta}{1+\eta}. \quad (89)$$

We see that the Berry phases in two blocks have opposite signs. For $\eta \ll 1$, we have $\Gamma_B^{\rm I} = -\Gamma_B^{\rm II} \approx 2\pi\eta$. In the opposite limit $1-\eta \ll 1$, we get $\Gamma_B^{\rm I} = -\Gamma_B^{\rm II} \approx \pi - \pi(1-\eta)/2$.

Next, we use Eq. (89) to clarify the underlying physics of the results obtained in the previous sections. Since we have already presented the rigorous derivations, in this section we will limit ourselves to the qualitative estimates omitting coefficients on the order of unity. The estimates are valid in the diffusion approximation, so that we will only discuss the regions $\eta \ll 1$ and $1-\eta \ll 1$.

Let us start with the case of zero magnetic field. Redrawing in the momentum space coherent scattering processes shown in Figs. 1 and 2, and taking into account that the amplitudes of the trajectories shown by dashed lines should be complex conjugated, one easily finds that the total geometrical phase factor entering the return probability $W(\phi)$ is given by

$$e^{i\theta} = e^{i\Gamma_B(1+2n)}, \quad (90)$$

where $-\infty < n < \infty$ is an integer number (winding number) and Γ_B equals $\Gamma_B^{\rm I}$ or $\Gamma_B^{\rm II}$. For a given value of ϕ, the winding number strongly fluctuates due to the diffusive nature of the particle motion. In the diffusion approximation, the distribution of the directions of the particle momentum obeys the diffusion law $P(\phi_{\mathbf{k}}) = \exp(-\phi_{\mathbf{k}}^2/4\gamma t)/\sqrt{4\pi\gamma t}$ (since we present order-of-magnitude estimates only, we do not distinguish between total and transport scattering rates). We used here the extended Fermi surface, assuming that $-\infty < \phi_{\mathbf{k}} < \infty$. Putting $\phi_{\mathbf{k}} \approx 2\pi n$ and averaging Eq. (90) over n with the function $P(\phi_{\mathbf{k}}) = P(2\pi n)$, we find

$$\langle e^{i\theta}\rangle \propto \begin{cases} \exp(-\eta^2\gamma t) & \text{for} \quad \eta \to 0, \\ -\exp[-(1-\eta)^2\gamma t] & \text{for} \quad \eta \to 1. \end{cases} \quad (91)$$

Equation (91) allows one to interpret the finite gap in the Cooperon propagator in terms of decay of the averaged Berry-phase factor due to the diffusive fluctuations of the winding number. Indeed, multiplying Eq. (91) with the product of the diffusive return probability $1/Dt$ (here $D \sim v_F^2/\gamma$) and the decoherence factor $\exp(-t/\tau_\varphi)$, and integrating over t from $t \sim 1/\gamma$ to $t = \infty$, one easily reproduces logarithms entering Eqs. (69) and (70). It is worth noting that the negative sign in front of the exponent in the second line of Eq. (91) is responsible for the change of WL to WAL and also arises due to the geometrical reasons (because $\Gamma_B = \pi$ for $\eta = 1$).

The approach based on the Berry-phase picture also allows one to give a transparent physical interpretation of the low-field linear magnetoresistance. For $B \neq 0$, the return probability acquires the phase factor [63] $\exp(2ieBS/\hbar c) = \exp(iS/l_B^2)$ in addition to the Berry-phase factor. Here, S is the algebraic area covered by the particle while propagating along the closed loop. Let us assume that $D\tau_\varphi \ll l_B^2$. We also assume that $1/\tau_\varphi \gg \eta^2\gamma$ ($\Gamma \gg \eta^2$) in the region $\eta \ll 1$ and $1/\tau_\varphi \gg$

$(1-\eta)^2\gamma$ [$\Gamma \gg (1-\eta)^2$] in the region $1-\eta \ll 1$. In this case, both phase factors can be expanded in the Taylor series. As a next step, one should average over diffusion motion of the particle. Evidently,

$$\langle S\rangle = 0, \quad \langle S^2\rangle \sim (D\tau_\varphi)^2, \tag{92}$$

$$\langle n\rangle = 0, \quad \langle n^2\rangle \sim \tau_\varphi\gamma. \tag{93}$$

It is also clear physically that some correlations between S and n should exist. To calculate the correlation function $\langle nS\rangle$ at a given time t ($t \sim \tau_\varphi \gg \gamma^{-1}$), we write

$$nS \approx \frac{\phi(t)}{2\pi}\int_0^t dt_2 \int_0^{t_2} dt_1 v_F^2 \sin[\phi(t_2)-\phi(t_2)]/2, \tag{94}$$

and average by functional integration over $\{D\phi\}$ with the weight $\exp(-\int_0^t \dot\phi^2 dt\,\tau)$. Standard calculation yields

$$\langle nS\rangle \sim D\tau_\varphi. \tag{95}$$

Magnetoconductivity is estimated as

$$\delta\sigma(b)-\delta\sigma(0) \propto -e^{i\Gamma_B}\left\langle -S^2/2l_B^4 - 2\Gamma_B nS/l_B^2\right\rangle. \tag{96}$$

Using Eqs. (92) and (95), we find

$$\delta\sigma^{\mathrm{I,II}}(b)-\delta\sigma^{\mathrm{I,II}}(0) \propto \begin{cases} b^2/b_*^2 \pm \eta b/b_* & \text{for} \quad \eta\to 0, \\ -b^2/b_*^2 \pm (1-\eta)b/b_* & \text{for} \quad \eta\to 1, \end{cases} \tag{97}$$

where signs + and − stand for I and II blocks, respectively, and $b_* \sim \Gamma$ under approximations used in this subsection. Hence, we reproduce by the order of magnitude the low-field magnetoconductivity given by Eqs. (77) and (79). We see that within the Berry-phase formalism, linear-in-b terms appear due to correlation between S and n.

V. BLOCK MIXING

A. Zero magnetic field $B = 0$.

Let us now assume that blocks are mixed by weak perturbation. We consider only positive energies $E > M$, so that the Hilbert space is limited to the states $\chi_{\mathbf{k}}^{(\mathrm{I},+)}, \chi_{\mathbf{k}}^{(\mathrm{II},+)}$. It is convenient to redefine these states multiplying $\chi_{\mathbf{k}}^{(\mathrm{I},+)}$ by a phase factor $e^{i\phi_{\mathbf{k}}}$. Hence, the spinors corresponding to the states in two blocks with positive energies are chosen as follows:

$$|\mathrm{I}_{\mathbf{k}}\rangle = \frac{1}{\sqrt{1+\eta}}\begin{pmatrix} e^{i\phi}\\ \sqrt{\eta}\\ 0\\ 0\end{pmatrix}, \quad |\mathrm{II}_{\mathbf{k}}\rangle = \frac{1}{\sqrt{1+\eta}}\begin{pmatrix} 0\\ 0\\ 1\\ -\sqrt{\eta}e^{i\phi}\end{pmatrix}. \tag{98}$$

The general form of a perturbation which mixes blocks and conserves the time-reversal symmetry is presented in Ref. [44]. In the following, we assume the simplest form of the mixing potential:

$$\hat V = V(\mathbf{r})\begin{bmatrix} 1 & 0 & 0 & -\Delta\\ 0 & 1 & \Delta & 0\\ 0 & \Delta^* & 1 & 0\\ -\Delta^* & 0 & 0 & 1\end{bmatrix}, \tag{99}$$

where $V(\mathbf{r})$ is a short-range potential with the correlation function given by Eq. (20) and Δ is a parameter responsible for the block mixing. In the following, we assume that Δ is small and real:

$$\Delta \ll 1, \quad \Delta = \Delta^*.$$

The potential (99) obeys the symmetry $\hat V = \hat U \hat V^* \hat U^{-1}$, where

$$\hat U = \begin{bmatrix} 0 & 0 & -i & 0\\ 0 & 0 & 0 & -i\\ i & 0 & 0 & 0\\ 0 & i & 0 & 0\end{bmatrix}, \quad \hat U\hat U^* = -1. \tag{100}$$

The matrix elements of $\hat V$ read as

$$\begin{aligned} \langle \mathrm{I}_{\mathbf{k}}|\hat V|\mathrm{I}_{\mathbf{k}'}\rangle &= V_{\mathbf{k}\mathbf{k}'}\frac{\eta + e^{i(\phi'-\phi)}}{1+\eta},\\ \langle \mathrm{II}_{\mathbf{k}}|\hat V|\mathrm{II}_{\mathbf{k}'}\rangle &= V_{\mathbf{k}\mathbf{k}'}\frac{1+\eta e^{i(\phi'-\phi)}}{1+\eta},\\ \langle \mathrm{I}_{\mathbf{k}}|\hat V|\mathrm{II}_{\mathbf{k}'}\rangle &= \langle \mathrm{II}_{\mathbf{k}}|\hat V|\mathrm{I}_{\mathbf{k}'}\rangle\\ &= V_{\mathbf{k}\mathbf{k}'}\frac{1+e^{i(\phi'-\phi)}}{1+\eta}\Delta\sqrt{\eta}. \end{aligned} \tag{101}$$

Using these equations, one can derive the equation for the Cooperon using standard diagrammatic rules. However, one can see that this representation is inconvenient because the single-particle Green's functions (calculated in the self-consistent Born approximation) turn out to be matrices 2×2. It is more convenient to make a unitary transformation which diagonalizes the Green's functions. Such a transformation looks like

$$|1_{\mathbf{k}}\rangle = \frac{|\mathrm{I}_{\mathbf{k}}\rangle + |\mathrm{II}_{\mathbf{k}}\rangle}{\sqrt{2}}, \quad |2_{\mathbf{k}}\rangle = \frac{|\mathrm{I}_{\mathbf{k}}\rangle - |\mathrm{II}_{\mathbf{k}}\rangle}{\sqrt{2}}. \tag{102}$$

Derivation of kinetic equation for the Cooperon in the new basis is presented in Appendix C 1. This equation has a matrix form

$$\begin{aligned} &[1/\tau_\phi + i\mathbf{q}\mathbf{v}_F + \hat\gamma_D]\hat C_{\mathbf{q}}(\phi,\phi_0)\\ &\quad = \int \frac{d\phi'}{2\pi}\hat\gamma_C(\phi-\phi')\hat C_{\mathbf{q}}(\phi',\phi_0) + \gamma\hat I\delta(\phi-\phi_0), \end{aligned} \tag{103}$$

where $\hat I$ is the unit matrix 4×4, and the matrix $\hat\gamma_C(\phi)$ contains three angular harmonics

$$\hat\gamma_C(\phi) = \hat\gamma_0 + \hat\gamma_{-1}e^{-i\phi} + \hat\gamma_{-2}e^{-2i\phi}. \tag{104}$$

The expressions for matrices $\hat\gamma_0, \hat\gamma_{-1}, \hat\gamma_{-2}$, and $\hat\gamma_D$ are presented in the Appendix C 1.

The conductivity correction is expressed in terms of the matrix return probability as follows:

$$\delta\sigma_{\mathrm{tot}} = -\frac{e^2}{\hbar}\frac{l_{tr}^2}{\gamma}\int\frac{d\phi}{2\pi}\mathrm{Tr}[\hat\gamma(\pi-\phi)\hat\xi\hat W(\phi)](1+\cos\phi), \tag{105}$$

where

$$\hat W(\phi-\phi_0) = \int\frac{d^2\mathbf{q}}{(2\pi)^2}\hat C_{\mathbf{q}}(\phi,\phi_0) \tag{106}$$

and

$$\hat{\xi} = \begin{bmatrix} 1 & 0 & 0 & 0 \\ 0 & 1 & 0 & 0 \\ 0 & 0 & -1 & 0 \\ 0 & 0 & 0 & 1 \end{bmatrix}. \tag{107}$$

Expanding $\hat{W}(\phi)$ in the Fourier series

$$\hat{W}(\phi) = \frac{1}{2\pi l^2} \sum_{M=-\infty}^{\infty} \hat{w}_M e^{i(M-1)\phi}, \tag{108}$$

we can write the conductivity correction in a form similar to Eq. (68):

$$\begin{aligned} \delta\sigma_{\rm tot} = -\frac{e^2}{2\pi\hbar}\left(\frac{l_{tr}}{l}\right)^2 \frac{1}{\gamma}{\rm Tr}\Bigg[& \frac{\hat{\gamma}_{-2}}{2}\hat{\xi}\hat{w}_{-2} \\ & + \left(\hat{\gamma}_{-2} - \frac{\hat{\gamma}_{-1}}{2}\right)\hat{\xi}\hat{w}_{-1} - \left(\hat{\gamma}_{-1} - \frac{\hat{\gamma}_0 + \hat{\gamma}_{-2}}{2}\right)\hat{\xi}\hat{w}_0 \\ & + \left(\hat{\gamma}_0 - \frac{\hat{\gamma}_{-1}}{2}\right)\hat{\xi}\hat{w}_1 + \frac{\hat{\gamma}_0}{2}\hat{\xi}\hat{w}_2\Bigg]. \end{aligned} \tag{109}$$

Since $\Delta \ll 1$, the matrices standing in front of $\hat{w}_n$ can be calculated for $\Delta = 0$. They are written in Appendix C 2.

For $q = 0$, Eq. (103) is easily solved by expansion $\hat{C}_{\mathbf{q}}(\phi,\phi_0)$ in the Fourier series over $\exp(iM\phi)$. Doing so, one can find "masses" of the diffusive modes which are given by the eigenvalues of the matrices $\hat{\gamma}_D - \hat{\gamma}_M$ $(M = 0,-1,-2)$. These matrices are presented in Appendix C 3. For $q \neq 0$, different harmonics couple with each other. In the diffusion approximation, when $ql \ll 1$, the coupling is weak and the mode $e^{iM\phi}$ is only effectively coupled with the nearest modes $e^{i(M\pm1)\phi}$. The main formulas describing diffusion approximation in the presence of the block mixing are quite similar to those obtained in Sec. III C. We present them in Appendix C 4.

Next, we demonstrate that the interblock mixing leads to appearance of two additional singular modes which do not show up in the absence of mixing. To this end, let us analyze eigenvalues of the matrix $\hat{\gamma}_D - \hat{\gamma}_{-1}$. This matrix is diagonal, so that its eigenvalues are given by the diagonal elements. The matrix element $(\hat{\gamma}_D - \hat{\gamma}_{-1})_{44}$ is exactly equal to zero, while the element $(\hat{\gamma}_D - \hat{\gamma}_{-1})_{33} = 4\eta\Delta^2$ turns to zero for $\Delta = 0$ when interblock transitions are absent. Hence, there are two modes which are singular (gapless for any η) in the limit $\Delta \to 0$. We will call these modes interblock singular modes (ISM). In Appendix D, we present calculation of the contribution of ISM to the conductivity and also find equations describing limiting cases $\eta \to 0$ or 1. In the following, we summarize the results of the calculations. For $b = 0$, conductivity correction coming from ISM reads as

$$\delta\sigma_{\rm ISM} = \frac{e^2}{4\pi^2\hbar}\left[\ln\left(\frac{1}{\Gamma}\right) - \ln\left(\frac{1}{\Gamma + 4\Delta^2\eta/(1+\eta^2)}\right)\right]. \tag{110}$$

We see that contributions of two modes exactly cancel each other in the limit $\Delta \to 0$. This explains why these modes do not show up in the model of independent blocks. In the limit $\Gamma \to 0$, the first logarithm dominates. It represents a standard singlet contribution responsible for weak antilocalization.

Importantly, Eq. (110) is valid in the whole interval $0 < \eta < 1$ because the applicability of the diffusion approximation which was used in our derivation is guaranteed by the smallness of dimensionless gaps of the diffusive modes: $\Gamma \ll 1$ and $\Gamma + 4\Delta^2\eta/(1+\eta^2) \ll 1$. Next, we notice that other modes, discussed in previous sections, are not strongly affected by block mixing provided that η is not too close to 0 or 1. This allows one to find analytical expression for total conductivity correction valid in the whole interval $0 < \eta < 1$, except narrow regions near points $\eta = 0$ and 1:

$$\delta\sigma_{\rm tot} = \delta\sigma_{\rm ISM} + 2\delta\sigma_{\rm II}, \tag{111}$$

where $\delta\sigma_{\rm II}$ is given by Eq. (68) with w_n determined by Eq. (41) and coefficient 2 in front of $\delta\sigma_{\rm II}$ accounts for the contribution of two blocks. To avoid confusion, we stress again that adding expression for $\delta\sigma_{\rm ISM}$ obtained in the diffusion approximation to the ballistic contribution $2\delta\sigma_{\rm II}$ is well controlled because for small Δ and Γ gaps of ISM are much smaller than γ.

B. Nonzero magnetic field $B \neq 0$.

In a finite magnetic field, the contribution of ISM becomes

$$\begin{aligned} \delta\sigma_{\rm ISM} &= -\frac{e^2}{4\pi^2\hbar} \\ &\quad \times \sum_{n=0}^{N}\left[\frac{|b|}{|b|(n+1/2)+A_1} - \frac{|b|}{|b|(n+1/2)+A_2}\right] \\ &= -\frac{e^2}{4\pi^2\hbar}\left[h\left(|b|,A_1\right) - h\left(|b|,A_2\right)\right], \end{aligned} \tag{112}$$

where

$$A_1 = \left(\Gamma + \frac{4\eta\Delta^2}{1+\eta^2}\right)\frac{1+\eta^2-\eta}{2(1+\eta^2)}, \quad A_2 = \Gamma\frac{1+\eta^2-\eta}{2(1+\eta^2)}. \tag{113}$$

Next, we write

$$\begin{aligned} \Delta\sigma_{\rm ISM} &= \delta\sigma_{\rm ISM}(b) - \delta\sigma_{\rm ISM}(0) \\ &= \frac{e^2}{4\pi^2\hbar}[h(|b|,A_2) - h(|b|,A_1) - h(0,A_2) + h(0,A_1)] \end{aligned} \tag{114}$$

and use Eq. (75) to find asymptotes of Eq. (114) for the case $\eta\Delta^2 \lesssim \Gamma$:

$$\begin{aligned} \Delta\sigma_{\rm ISM} \approx -\frac{e^2}{4\pi^2\hbar} \\ \times \begin{cases} \frac{b^2}{6}\frac{(1+\eta^2)^2}{(1+\eta^2-\eta)^2}\left[\frac{1}{\Gamma^2} - \frac{1}{(\Gamma+\frac{4\eta\Delta^2}{1+\eta^2})^2}\right] & \text{for} \quad |b| \ll \Gamma, \\ -\frac{\pi^2\eta\Delta^2(1+\eta^2-\eta)}{(1+\eta^2)^2|b|} & \text{for} \quad |b| \gg \Gamma. \end{cases} \end{aligned} \tag{115}$$

For stronger interblock coupling $\eta\Delta^2 \gg \Gamma$, we get

$$\Delta\sigma_{\rm ISM} \approx -\frac{e^2}{4\pi^2\hbar}\begin{cases}\frac{b^2}{6}\frac{(1+\eta^2)^2}{(1+\eta^2-\eta)^2\Gamma^2} & \text{for} \quad |b| \ll \Gamma,\\ \ln\left(\frac{|b|}{\Gamma}\right) - \frac{b^2}{96}\frac{(1+\eta^2)^4}{(1+\eta^2-\eta)^2\eta^2\Delta^4} & \text{for} \quad \Gamma \ll |b| \ll \eta\Delta^2,\\ -\frac{\pi^2\eta\Delta^2(1+\eta^2-\eta)}{(1+\eta^2)^2|b|} - \ln\left(\frac{\Gamma}{\eta\Delta^2}\right) & \text{for} \quad |b| \gg \eta\Delta^2.\end{cases} \tag{116}$$

The total conductivity correction reads as

$$\delta\sigma_{\rm tot} = \delta\sigma_{\rm ISM} + \delta\sigma_{\rm I} + \delta\sigma_{\rm II}, \tag{117}$$

where $\delta\sigma_{\rm I,II}$ are given by Eq. (68) with w_n determined by Eqs. (51) and (82), respectively (see Sec. IV B). Equation (117) yields the most general expression for conductivity correction in magnetic field. Just in the absence of field, expression $\delta\sigma_{\rm ISM}(b)$ was found in the diffusion approximation, while $\delta\sigma_{\rm I}$ and $\delta\sigma_{\rm II}$ are calculated by using exact ballistic formulas. Such an approach is well controlled for small Δ and Γ provided that η is not too close to 0 or 1.

Let us now consider the behavior of the conductivity correction near points $\eta = 0$ and 1. At zero field, in the absence of block mixing, the total conductivity correction is given by Eqs. (69) and (70), respectively, multiplied by a factor 2 which accounts for the contribution of the block I. Block mixing slightly modifies these equations because neglect of Δ in $\delta\sigma_{\rm I}$ and $\delta\sigma_{\rm II}$ is no longer justified. On the other hand, calculation of conductivity near these points can be essentially simplified because these are the points where the diffusion approximation works well.

(a) $\eta \to 0$. As shown in Appendix D, in the presence of the block mixing instead of Eq. (69) (multiplied by the factor 2), we get the following equation:

$$\delta\sigma_\eta \approx -\frac{e^2}{2\pi^2\hbar}\ln\left(\frac{1}{\Gamma+\eta^2+2\eta\Delta^2}\right), \tag{118}$$

which accounts for two weakly mixed blocks at $b = 0$. The total conductivity is given by the sum of $\delta\sigma_{\rm ISM}$ and $\delta\sigma_\eta$:

$$\begin{aligned}\delta\sigma_{\rm tot} &= \delta\sigma_\eta + \delta\sigma_{\rm ISM}\\ &\approx \frac{e^2}{4\pi^2\hbar}\left[\ln\left(\frac{1}{\Gamma}\right) - \ln\left(\frac{1}{\Gamma+4\Delta^2\eta}\right)\right.\\ &\quad \left. - 2\ln\left(\frac{1}{\Gamma+\eta^2+2\eta\Delta^2}\right)\right].\end{aligned} \tag{119}$$

This equation is valid, provided that $\eta \ll 1$. In the interval $\Delta^2 \ll \eta \ll 1$ it matches with Eq. (111).

The variation of the total conductivity correction with the magnetic field $\Delta\sigma_{\rm tot}(b) = \delta\sigma_{\rm tot}(b) - \delta\sigma_{\rm tot}(0)$ is presented as a sum of two terms:

$$\Delta\sigma_{\rm tot} = \Delta\sigma_{\rm ISM} + \Delta\sigma_\eta \tag{120}$$

where $\Delta\sigma_{\rm ISM}$ is given by Eqs. (114)–(116), whereas

$$\begin{aligned}\Delta\sigma_\eta &= \delta\sigma_\eta(b) - \delta\sigma_\eta(0)\\ &= -\frac{e^2}{4\pi^2\hbar}\left[h\left(|b|,\frac{\Gamma+\eta^2-\eta b+2\eta\Delta^2}{2}\right) + h\left(|b|,\frac{\Gamma+\eta^2+\eta b+2\eta\Delta^2}{2}\right) - 2h\left(0,\frac{\Gamma+\eta^2+2\eta\Delta^2}{2}\right)\right]\\ &\approx -\frac{e^2}{2\pi^2\hbar}\begin{cases}-\frac{b^2}{6}\frac{1}{(\Gamma+\eta^2+2\eta\Delta^2)^2} & \text{for} \quad |b| \ll \Gamma+\eta^2+2\eta\Delta^2,\\ \ln\left(\frac{\Gamma+\eta^2+2\eta\Delta^2}{|b|}\right) & \text{for} \quad |b| \gg \Gamma+\eta^2+2\eta\Delta^2.\end{cases}\end{aligned} \tag{121}$$

The low-field asymptotic of $\Delta\sigma_{\rm tot}$ deserves special attention. From Eqs. (115) and (121), we find for $|b| \to 0, \eta \ll 1$

$$\Delta\sigma_{\rm tot} \approx \frac{e^2b^2}{12\pi^2\hbar}\left[\frac{1}{(\Gamma+\eta^2+2\eta\Delta^2)^2} - \frac{4\eta\Delta^2(\Gamma+2\eta\Delta^2)}{\Gamma^2(\Gamma+4\eta\Delta^2)^2}\right]. \tag{122}$$

We see that coefficient in the square brackets changes sign with increasing of η or Δ. Consequently, the magnetoconductivity also changes sign and becomes negative.

(b) $\eta \to 1$. Instead of Eq. (70) (multiplied by the factor 2), we get the following equation:

$$\delta\sigma_{1-\eta} = \frac{e^2}{4\pi^2\hbar}\left[\ln\left(\frac{1}{\Gamma+(1-\eta)^2/2}\right) + \ln\left(\frac{1}{\Gamma+(1-\eta)^2/2+2\Delta^2}\right)\right], \tag{123}$$

which should be added to $\delta\sigma_{\rm ISM}$:

$$\begin{aligned}\delta\sigma_{\rm tot} &= \delta\sigma_{1-\eta} + \delta\sigma_{\rm ISM}\\ &\approx \frac{e^2}{4\pi^2\hbar}\left[\ln\left(\frac{1}{\Gamma}\right) - \ln\left(\frac{1}{\Gamma+2\Delta^2}\right) + \ln\left(\frac{1}{\Gamma+(1-\eta)^2/2+2\Delta^2}\right) + \ln\left(\frac{1}{\Gamma+(1-\eta)^2/2}\right)\right].\end{aligned} \tag{124}$$

This equation for zero-field correction is valid, provided that $1-\eta \ll 1$. In the interval $\Delta^2 \ll 1-\eta \ll 1$, it matches with Eq. (111).

The variation of the total conductivity correction with the magnetic field is written as

$$\Delta\sigma_{\rm tot} = \Delta\sigma_{\rm ISM} + \Delta\sigma_{1-\eta}, \tag{125}$$

where $\Delta\sigma_{\rm ISM}$ is given by Eqs. (114)–(116), whereas

$$\begin{aligned}\Delta\sigma_{1-\eta} &= \delta\sigma_{1-\eta}(b) - \delta\sigma_{1-\eta}(0)\\ &= \frac{e^2}{8\pi^2\hbar}\left\{h\left[|b|,\frac{\Gamma+(1-\eta)^2/2+2b(1-\eta)}{4}\right]+h\left[|b|,\frac{\Gamma+(1-\eta)^2/2+2b(1-\eta)+2\Delta^2}{4}\right]\right.\\ &\quad +h\left[|b|,\frac{\Gamma+(1-\eta)^2/2-2b(1-\eta)}{4}\right]+h\left[|b|,\frac{\Gamma+(1-\eta)^2/2-2b(1-\eta)+2\Delta^2}{4}\right]\\ &\quad \left.-2h\left[0,\frac{\Gamma+(1-\eta)^2/2}{4}\right]-2h\left[0,\frac{\Gamma+(1-\eta)^2/2+2\Delta^2}{4}\right]\right\}\\ &\approx \frac{e^2}{4\pi^2\hbar}\begin{cases}-\frac{2b^2}{3}\left\{\frac{1}{[\Gamma+\frac{(1-\eta)^2}{2}]^2}+\frac{1}{[\Gamma+\frac{(1-\eta)^2}{2}+2\Delta^2]^2}\right\} & \text{for}\quad |b|\to 0,\\ \ln\left\{\frac{[\Gamma+\frac{(1-\eta)^2}{2}][\Gamma+\frac{(1-\eta)^2}{2}+2\Delta^2]}{b^2}\right\} & \text{for}\quad |b|\gg\Gamma+(1-\eta)^2/2+2\Delta^2.\end{cases}\end{aligned} \tag{126}$$

C. Crossover between ensembles

Let us discuss results obtained in Secs. V A and V B in the context of crossover between orthogonal and symplectic ensembles. For an arbitrary value of η between 0 and 1 and $\Delta \neq 0$, all symmetries are broken except time-reversal symmetry (see Ref. [44] for detailed discussion of symmetries existing in the system), so that in the absence of dephasing ($\Gamma = 0$) there exists only one gapless mode. This mode gives rise to antilocalizing conductivity correction described by the first logarithm in Eq. (110).

In the limit $\eta \to 0$, the spin degree of freedom is irrelevant, so that we have two copies of a system with orthogonal symmetry. Indeed, as seen from Eq. (119) for $\eta = 0$ we have two (due to the spin degeneracy) gapless modes yielding the WL correction to the conductivity [described by the last logarithm in Eq. (119)].

The case $\eta \to 1$ turns out to be more subtle. Indeed, one may expect that in this case all symmetries are broken because of the interblock transition, and one may conclude that there exists a single copy of a system with symplectic symmetry corresponding to a divergent (in the limit $\Gamma \to 0$) logarithm. However, such a conclusion is not supported by our calculations. Indeed, as seen from Eq. (124), in addition to always singular mode [one of the ISM described by the first term in Eq. (124)] there also exists a mode which becomes singular when η becomes exactly equal to 1. This mode corresponds to the last term in Eq. (124). In other words, for $\eta = 1$ there exist two copies of the symplectic ensembles instead of one expected. The physical explanation of this fact follows from analysis of the interblock matrix element. Specifically, from the last line of Eq. (C1) we see that in the limit $\eta \to 1$, the interblock matrix element

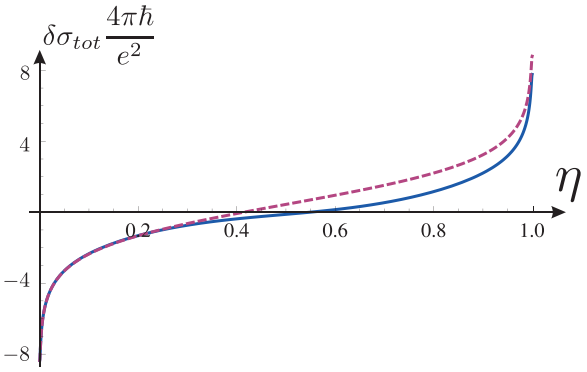

FIG. 3. (Color online) Conductivity correction as a function of η for infinite dephasing time. Dashed line: sum of two logarithms.

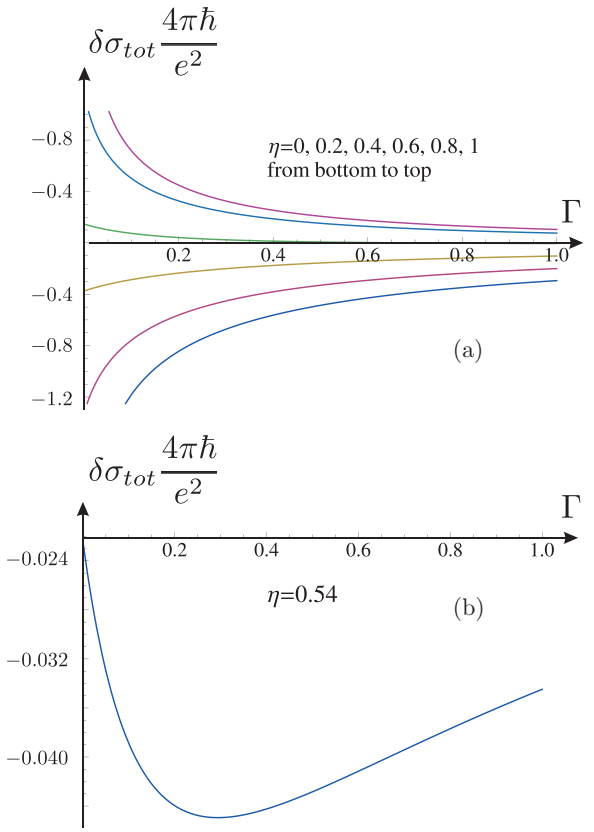

FIG. 4. (Color online) Conductivity correction as a function of dephasing rate for different values of η (a). Conductivity correction as a function of dephasing rate for $\eta = 0.54$ (b).

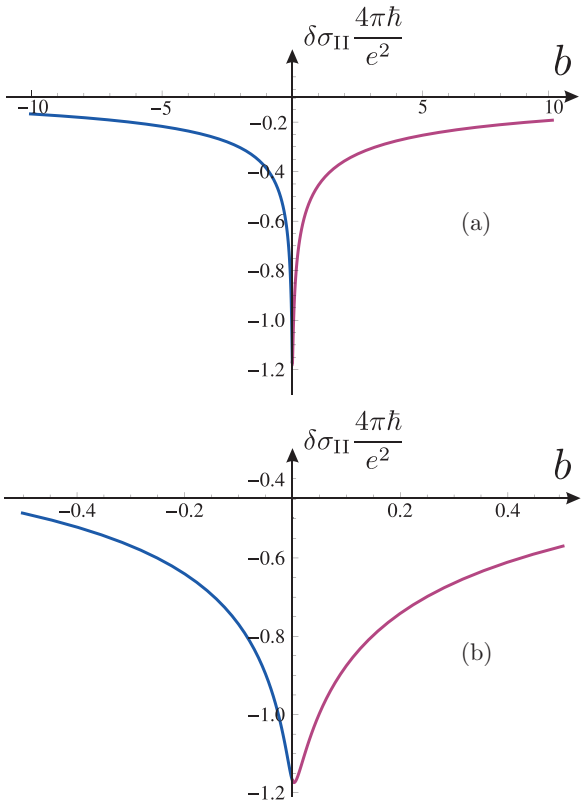

FIG. 5. (Color online) Magnetoconductivity within the block II in the intervals $-10 < b < 10$ (a) and $-0.5 < b < 0.5$ (b) for $\eta = 0.1, \Gamma = 0.01$.

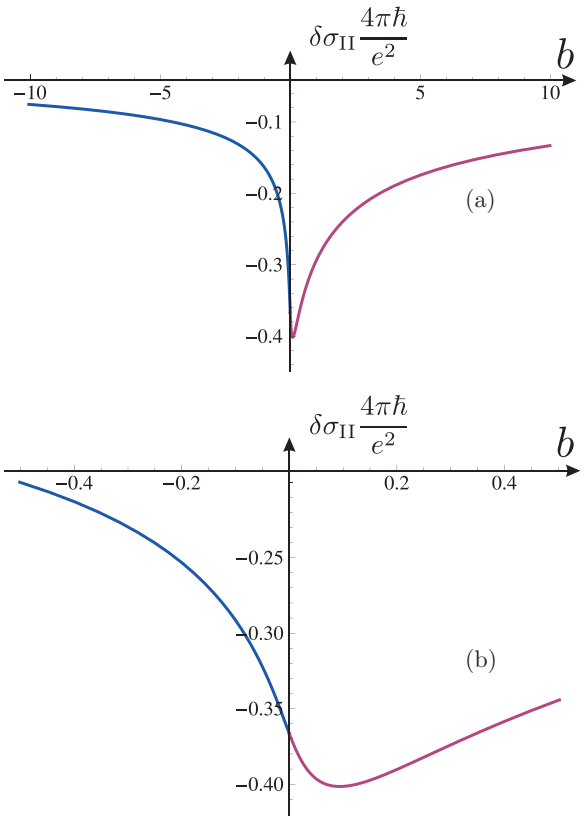

FIG. 6. (Color online) Magnetoconductivity within the block II in the intervals $-10 < b < 10$ (a) and $-0.5 < b < 0.5$ (b) for $\eta = 0.3, \Gamma = 0.01$.

exactly equals to zero, which means that perturbation (99) does not effectively mix blocks and, therefore, is not sufficient to break all symmetries except the time-reversal one. One may expect that this symmetry, however, is broken by the Rashba term arising in asymmetric quantum wells (see discussion and symmetry arguments in Refs. [44,45]), so that only single singular antilocalizing mode should survive. The detailed analysis of the interference correction in the presence of the Rashba coupling is out of the scope of this work.

VI. PLOTS OF THE CONDUCTIVITY CORRECTION

As seen from equations derived in the previous sections, interference correction at zero field as well as magnetoconductivity can be negative or positive depending on η, Γ, and Δ. In this section, we present corresponding pictures for different values of parameters.

A. Interference correction at zero field

In the absence of magnetic field and block mixing ($b = 0$, $\Delta = 0$), interference correction depends on two parameters, η and Γ : $\delta\sigma_{\rm tot} = \delta\sigma_{\rm tot}(\eta, \Gamma)$. In Fig. 3, the conductivity calculated by using Eqs. (41), (68), and (84) is plotted as a function of η for $\Gamma = 0$.

As seen, $\delta\sigma_{\rm tot}$ diverges at $\eta \to 0$ and 1, but remains finite for intermediate values of η. As a rough approximation, one can describe this dependence as a sum of two logarithmic terms, Eqs. (69) and (70) (multiplied by a factor 2 accounting for the contribution of the block II). This sum is shown by a dashed line.

With increasing Γ, correction is suppressed. This is illustrated in detail in Fig. 4(a), where the dependence of $\delta\sigma_{\rm tot}$ on Γ is plotted for different η increasing from bottom to top. Although at very large Γ correction always decays (by absolute value), the dependence of $\delta\sigma_{\rm tot}$ on Γ can be nonmonotonous for some intermediate values of η as shown in Fig. 4(b) for $\eta = 0.54$. Such a counterintuitive behavior arises due to the competition between localizing and antilocalizing contributions into interference correction (an analogous result was obtained for two-dimensional holes in semiconductor heterostructures [31]).

B. Magnetoconductivity in a single cone

In this section we present results of numerical simulations of magnetoconductivity in a single Dirac cone (block II) for $\Delta = 0$. In Figs. 5–10 we plotted dependence $\delta\sigma_{\rm II}(b)$ for fixed low dephasing rate, $\Gamma = 0.01$, and different η. In the upper panels of these pictures, $\delta\sigma_{\rm II}(b)$ is plotted within the interval $-10 < b < 10$, while in the lower panels we plot in more detail the low-field behavior $-0.5 < b < 0.5$. The most important information presented in these pictures is the asymmetry of the function $\delta\sigma_{\rm II}(b)$. (Such an asymmetry was previously found numerically in Ref. [46].) For η close to 0 and 1, the asymmetry is not that strong, however, even in

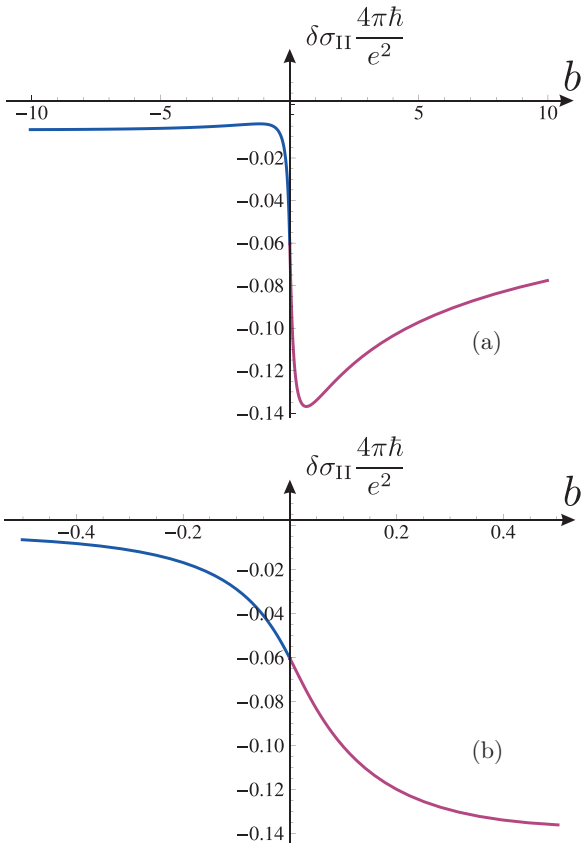

FIG. 7. (Color online) Magnetoconductivity within the block II in the intervals $-10 < b < 10$ (a) and $-0.5 < b < 0.5$ (b) for $\eta = 0.5, \Gamma = 0.01$.

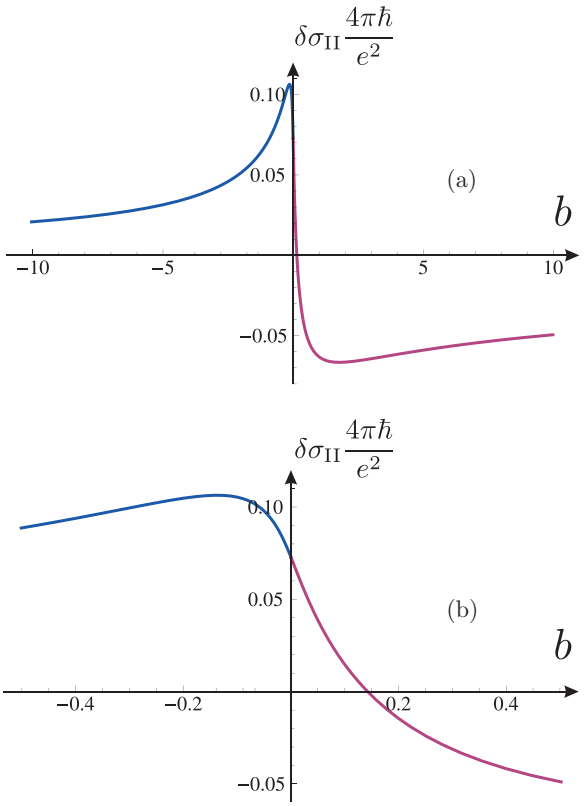

FIG. 8. (Color online) Magnetoconductivity within the block II in the intervals $-10 < b < 10$ (a) and $-0.5 < b < 0.5$ (b) for $\eta = 0.6, \Gamma = 0.01$.

these cases the peak of the magnetoconductivity is shifted away from the point $b = 0$. The most asymmetric curves are obtained for intermediate values of η [see, for example, plots of magnetoconductivity for $\eta = 0.5$ (Fig. 7) and $\eta = 0.6$ (Fig. 8)].

C. Total magnetoconductivity in the absence of the block mixing

In the previous section we demonstrated that in a single Dirac cone the magnetoconducitivty is a strongly asymmetric function of b. Taking into account contribution of the second block restores symmetry with respect to field inversion since, as mentioned above, $\delta\sigma_{\rm I}(b) = \delta\sigma_{\rm II}(-b)$ and, consequently, the total correction $\delta\sigma_{\rm tot} = \delta\sigma_{\rm I}(b) + \delta\sigma_{\rm II}(b)$ is an even function of b. As an example, let us consider the dependence of $\delta\sigma_{\rm tot}$ on b in the absence of block mixing ($\Delta = 0$) for $\Gamma = 0.01$ and different values of η (see Figs. 11–16). Comparing this curve with Figs. 5–10 plotted for the same parameters but for a single block, we see that adding of the contribution of the second block shifts the minimum of the conductivity back to the point $b = 0$.

The most interesting result is obtained for intermediate values of η. In particular, for $\eta = 0.5$, we see two minima in the low-field region symmetrical with respect to point $b = 0$.

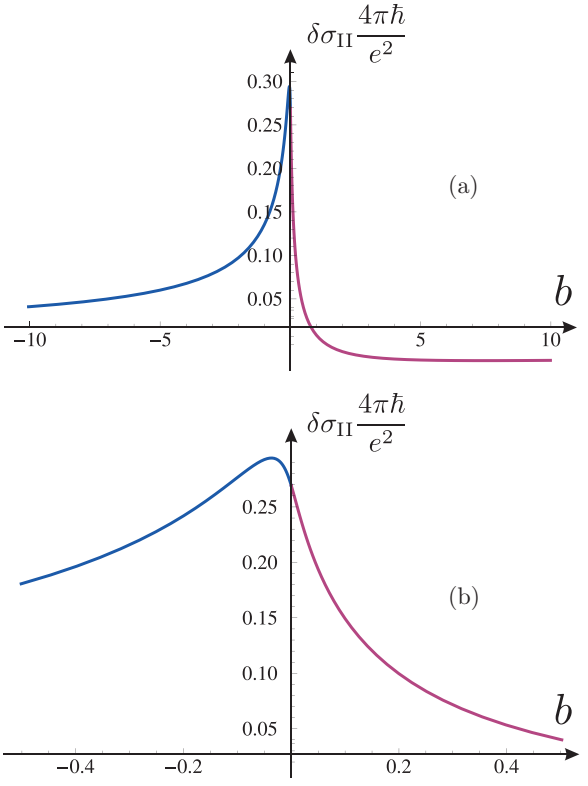

FIG. 9. (Color online) Magnetoconductivity within the block II in the intervals $-10 < b < 10$ (a) and $-0.5 < b < 0.5$ (b) for $\eta = 0.7, \Gamma = 0.01$.

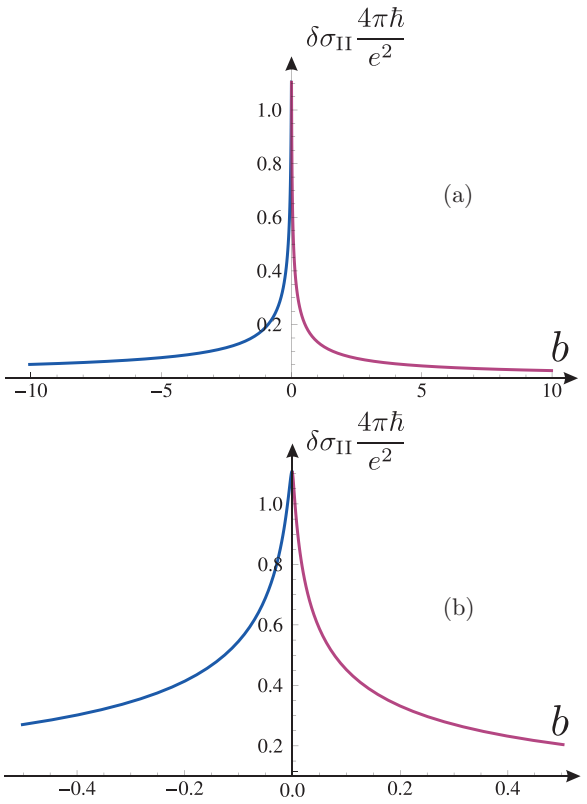

FIG. 10. (Color online) Magnetoconductivity within the block II in the intervals $-10 < b < 10$ (a) and $-0.5 < b < 0.5$ (b) for $\eta = 0.9, \Gamma = 0.01$.

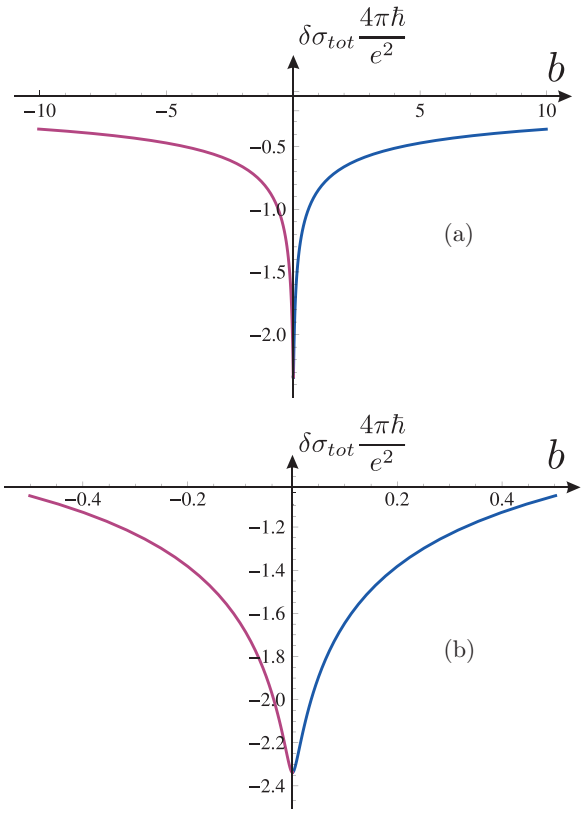

FIG. 11. (Color online) Total magnetoconductivity in the intervals $-10 < b < 10$ (a) and $-0.5 < b < 0.5$ (b) for η=0.1,Γ=0.01.

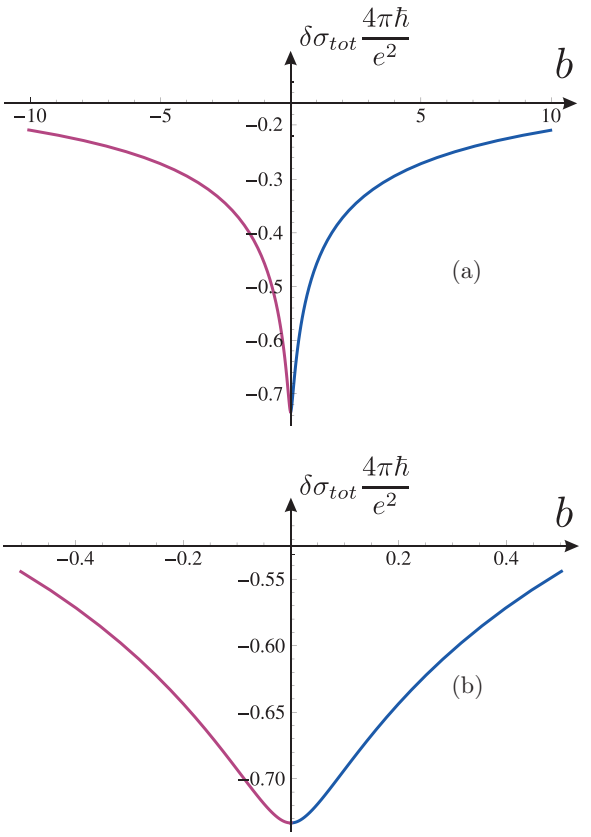

FIG. 12. (Color online) Total magnetoconductivity in the intervals $-10 < b < 10$ (a) and $-0.5 < b < 0.5$ (b) for η=0.3,Γ=0.01.

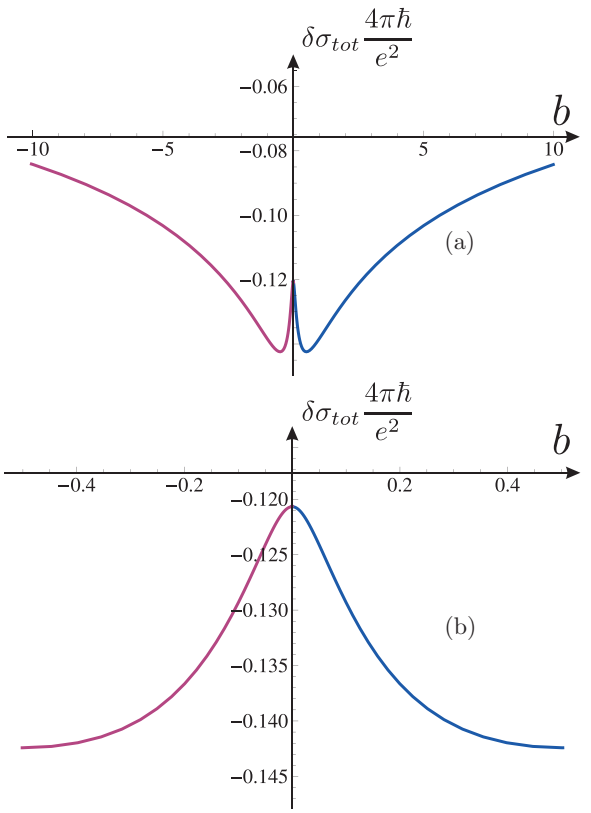

FIG. 13. (Color online) Total magnetoconductivity in the intervals $-10 < b < 10$ (a) and $-0.5 < b < 0.5$ (b) for η=0.5,Γ=0.01.

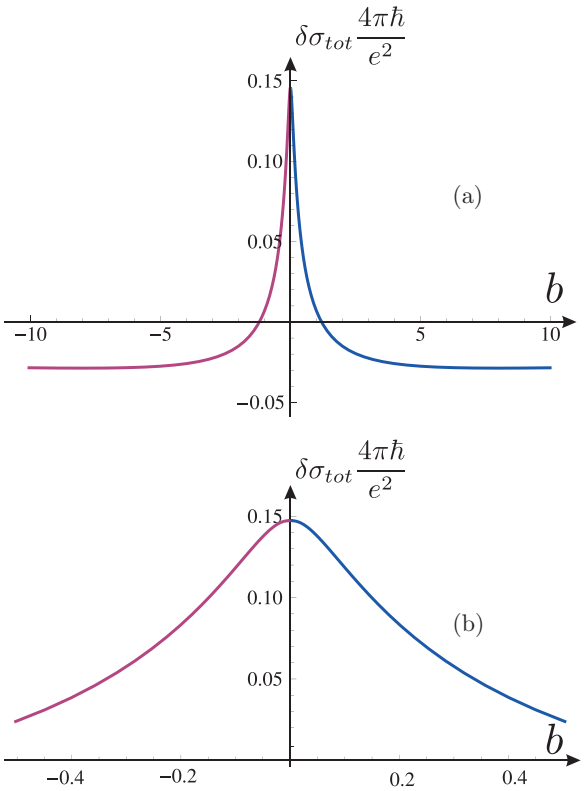

FIG. 14. (Color online) Total magnetoconductivity in the intervals $-10 < b < 10$ (a) and $-0.5 < b < 0.5$ (b) for $\eta = 0.6, \Gamma = 0.01$.

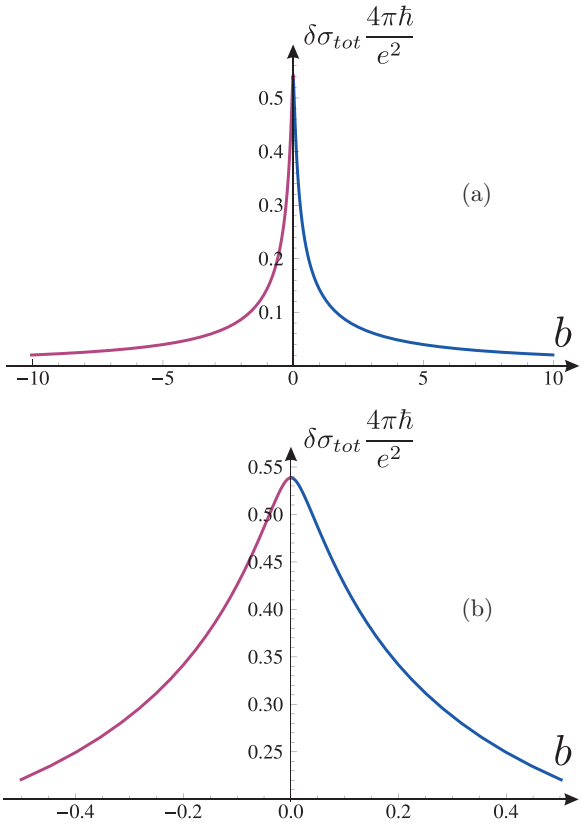

FIG. 15. (Color online) Total magnetoconductivity in the intervals $-10 < b < 10$ (a) and $-0.5 < b < 0.5$ (b) for $\eta = 0.7, \Gamma = 0.01$.

D. Total magnetoconductivity in the presence of the block mixing

In this section we present the plots for magnetoconductivity in the presence of the block mixing. As we mentioned in Sec. V, for weak coupling between blocks ($\Delta \ll 1$) one can use the diffusion approximation for calculation of the contribution of the ISM. This contribution should be added to the term $\delta\sigma_{\rm I} + \delta\sigma_{\rm II}$, where $\delta\sigma_{\rm I}$ and $\delta\sigma_{\rm II}$ can be calculated by using exact ballistic equations with $\Delta = 0$. Such an approach can be applied within the whole interval $0 < \eta < 1$ except vicinities of the points $\eta = 0$ and 1. At these special points, one can also obtain analytical results by using the diffusion approximation for all terms contributing to the conductivity correction $\delta\sigma_{\rm tot}$. Using the approach described above, we plotted in Fig. 17 total correction $\delta\sigma_{\rm tot}$ for different η both for the absence of the block mixing [$\Delta = 0$, see Fig. 17(a)] and for weak interblock coupling [$\Delta = 0.1$, see Fig. 17(b)]. Comparing these plots, we see that the main effect of the mixing is the appearance of the positive peak in the region of low b for $\eta \gtrsim 0.1$. This peak is most pronounced for $\eta = 0.3$. as shown in Fig. 18. Physically, low-field negative magnetoconductivity arises due to the contribution of ISM. The peak at $b = 0$ is well described by Eq. (112) [see also Eq. (122) and discussion after this equation].

E. Strong-field asymptotic of the conductivity

Finally, we present the results for the asymptotical behavior of the conductivity correction at sufficiently strong B, such that the magnetic length becomes much smaller than the mean-free path ($|b| \gg 1$). In this case, the main contribution to the quantum correction comes from the short electron trajectories involving scattering on untypical impurity configurations, namely, on the complexes of three impurities separated by untypical distance $l_B \ll l$ [59,60].

For simplicity, we neglect here block mixing and consider $\delta\sigma_{\rm II}$. As shown in Appendix E in the strong-field limit conductivity correction can be presented as

$$\delta\sigma_{\rm II} = \frac{e^2}{2\pi\hbar}\frac{l_B}{l}A_{\rm II}(\eta) \propto \frac{1}{\sqrt{b}}, \tag{127}$$

so that conductivity decays as a square root of the field: $\delta\sigma_{\rm II} \propto 1/\sqrt{|b|}$. The coefficient $A_{\rm II}(\eta)$ is different for the positive and negative b. Its analytical dependence is found in Appendix E. The plots of $A_{\rm II}(\eta)$ for positive and negative fields are shown in Fig. 19. Due to the property $\delta\sigma_{\rm I}(b) = \delta\sigma_{\rm II}(-b)$, Fig. 19 presents at the same time dependence of $A_{\rm I}(\eta)$ for negative and positive fields, respectively. The sum $A_{\rm I}(\eta) + A_{\rm II}(\eta)$ which determines asymptotical behavior of the total correction turns to zero at $\eta \approx 0.715$.

VII. SUMMARY

We have developed a microscopic theory of the quantum transport in spin-orbit metals realized in HgTe quantum wells away from the topological insulator phase. Our theory is applicable to a wide range of particle concentrations and describes the crossover between WL and WAL regimes. We

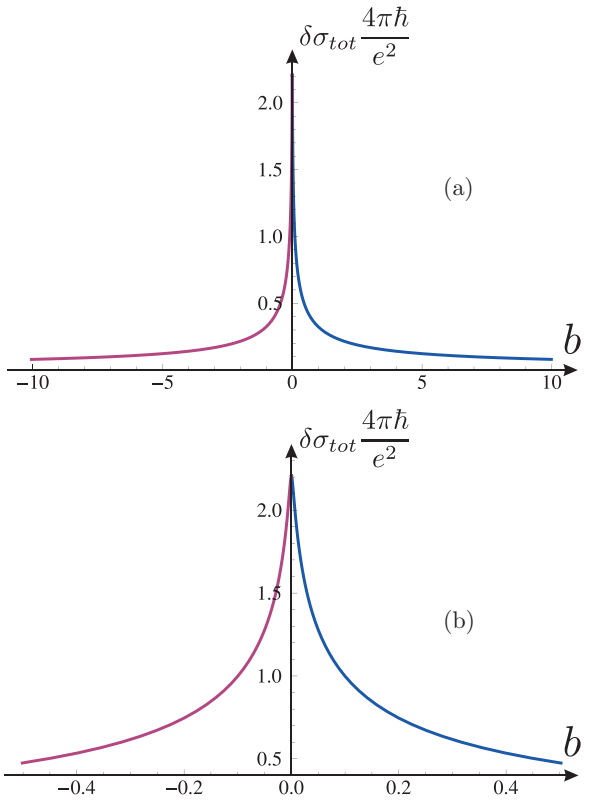

FIG. 16. (Color online) Total magnetoconductivity in the intervals $-10 < b < 10$ (a) and $-0.5 < b < 0.5$ (b) for $\eta = 0.9, \Gamma = 0.01$.

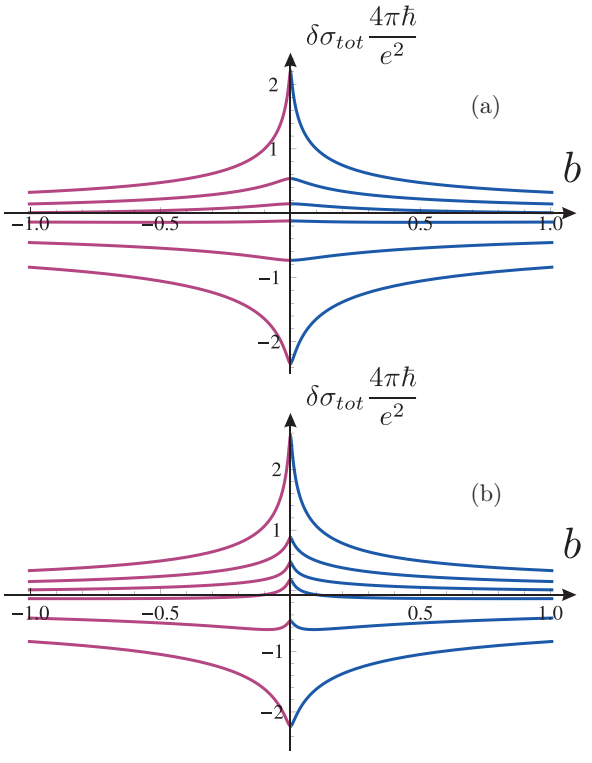

FIG. 17. (Color online) Conductivity correction as a function of b at $\Gamma = 0.01$ and different η ($\eta = 0.1, 0.3, 0.5, 0.6, 0.7, 0.9$) in the absence of the block mixing $\Delta = 0$ (a) and for weak mixing $\Delta = 0.1$ (b).

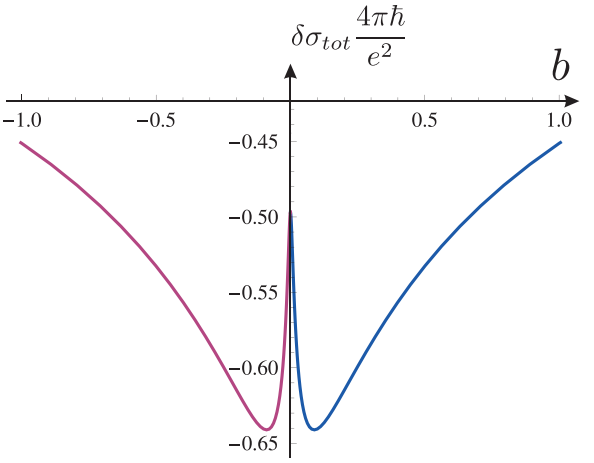

FIG. 18. (Color online) Conductivity correction as a function of b at $\Gamma = 0.001$, $\eta = 0.3$, $\Delta = 0.1$.

demonstrated that this crossover is governed by the single parameter η ($0 \leqslant \eta \leqslant 1$). All essential information about details of the spectrum and eigenfunctions at the Fermi energy is encoded in this parameter. Hence, our results are applicable not only to the HgTe quantum wells, but also to other systems governed by the generic Hamiltonian (1), in particular, to surfaces of 3D topological insulators [53], to massive Dirac fermions in graphene on the BN substrate [64], and to semiconductors with strong Rashba splitting of the spectrum [10].

We have found analytically an exact expression for the Cooperon propagator in magnetic field valid beyond the diffusion approximation. Using this equation, we have calculated the interference-induced magnetoresistance in a wide interval of magnetic fields. We found that the contributions of the two massive Dirac cones do not coincide, $\delta\sigma_{\rm I}(b) \neq \delta\sigma_{\rm II}(b)$, and both are asymmetric functions of the magnetic field: $\delta\sigma_{\rm I}(b) \neq \delta\sigma_{\rm I}(-b)$ and $\delta\sigma_{\rm II}(b) \neq \delta\sigma_{\rm II}(-b)$. Only the total conductivity correction $\delta\sigma_{\rm I} + \delta\sigma_{\rm II}$ is an even function of the magnetic field. Special attention was given to the low- and strong-field limits. In particular, we have found that each Dirac cone taken separately gives a linear contribution to the low-field magnetoresistance, whereas the total correction is parabolic in the limit $B \to 0$. In the opposite limit of large

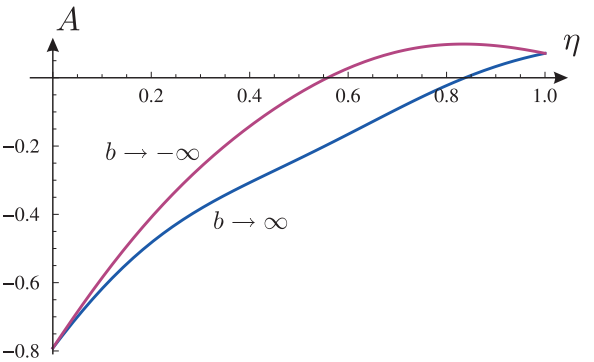

FIG. 19. (Color online) Coefficient A as a function of η for $b \to \infty$ (lower curve) and for $b \to -\infty$ (upper curve).

B, the magnetoresistance decays as $1/\sqrt{B}$ with the prefactor being a function of the electron concentration. We have also demonstrated that the block mixing gives rise to additional singular diffusive modes which do not show up in the absence of the mixing. One of these modes remains singular at $B = 0$ and $T = 0$ for arbitrary electron concentration and yields the WAL correction. This implies that any small but finite coupling between blocks turns the system into WAL regime at sufficiently low temperatures. We have shown that the quantum correction might change in nonmonotonous way both with the phase-breaking rate and with the magnetic field and that the block mixing might lead to an additional mechanism of the nonmonotonous magnetoresistance.

Finally, we note that the crossover from WL to WAL with increasing carrier concentration in HgTe-based quantum wells was already observed in a number of experiments [55–58]. Detailed analysis of experimental data is out of scope of this paper. It is worth, however, stressing that on the qualitative level our theoretical predictions for magnetoconductivity (see Fig. 17) are in a good agreement with experimental results (see Fig. 3 of Ref. [55]).

ACKNOWLEDGMENTS

We are grateful to N. Averkiev, C. Brüne, A. Germanenko, L. Golub, E. Hankiewicz, E. König, Z.D. Kvon, G. Minkov, A. Mirlin, M. Titov, and G. Tkachov for useful discussions. The work was supported by DFG within DFG SPP "Semiconductor spintronics" and DFG SPP "Topological insulators," by DFG CFN, by Grant No. FP7-PEOPLE-2013 of the EU IRSES network InterNoM, by RFBR, and by BMBF.

APPENDIX A: SOLUTION OF THE KINETIC EQUATION FOR THE COOPERON IN THE ABSENCE OF THE BLOCK MIXING

1. Zero magnetic field

Here, we find analytically rigorous solution of Eq. (37) valid beyond the diffusion approximation. As seen from this equation, the incoming term of the collision integral contains only three angular harmonics: $0, -1, -2$. This allows us to present the solution of Eq. (37) in the following form:

$$C_{\mathbf{Q}}(\phi,\phi_0) = \frac{C_0 + e^{i(\phi_{\mathbf{Q}}-\phi)}C_{-1} + e^{2i(\phi_{\mathbf{Q}}-\phi)}C_{-2} + \delta(\phi-\phi_0)}{1+\Gamma+i\mathbf{Qn}}, \tag{A1}$$

where the coefficients

$$C_0 = \frac{1}{1+\eta^2}\int \frac{d\phi}{2\pi} C_{\mathbf{Q}}(\phi,\phi_0), \tag{A2}$$

$$C_{-1} = \frac{2\eta}{1+\eta^2}\int \frac{d\phi}{2\pi} C_{\mathbf{Q}}(\phi,\phi_0)e^{i(\phi-\phi_{\mathbf{Q}})}, \tag{A3}$$

$$C_{-2} = \frac{\eta^2}{1+\eta^2}\int \frac{d\phi}{2\pi} C_{\mathbf{Q}}(\phi,\phi_0)e^{2i(\phi-\phi_{\mathbf{Q}})} \tag{A4}$$

do not depend on ϕ being the functions of ϕ_0 and $\phi_{\mathbf{Q}}$ only. Here, $\phi_{\mathbf{Q}}$ is the angle of the vector $\mathbf{Q}$. From Eqs. (A1)–(A4), we find a system of equations for C_0, C_{-1}, and C_{-2}:

$$\hat{M}\begin{bmatrix} C_0 \\ C_{-1} \\ C_{-2}\end{bmatrix} = \frac{1}{2\pi(1+\Gamma+i\mathbf{Qn}_0)}\begin{bmatrix} 1 \\ e^{i(\phi_0-\phi_{\mathbf{Q}})} \\ e^{2i(\phi_0-\phi_{\mathbf{Q}})}\end{bmatrix}. \tag{A5}$$

Here, matrix $\hat{M}$ and its elements are given, respectively, by Eqs. (42) and (43) of the main text. From Eqs. (A1), (A5), and (42), we find

$$C_{\mathbf{Q}}(\phi,\phi_0) = \frac{\delta(\phi-\phi_0)}{1+\Gamma+i\mathbf{Qn}} + \frac{1}{2\pi(1+\Gamma+i\mathbf{Qn})(1+\Gamma+i\mathbf{Qn}_0)} \times \begin{bmatrix} 1 \\ e^{i(\phi_{\mathbf{Q}}-\phi)} \\ e^{2i(\phi_{\mathbf{Q}}-\phi)}\end{bmatrix}^T \hat{M}^{-1}\begin{bmatrix} 1 \\ e^{i(\phi_0-\phi_{\mathbf{Q}})} \\ e^{2i(\phi_0-\phi_{\mathbf{Q}})}\end{bmatrix}, \tag{A6}$$

where $\mathbf{n} = (\cos\phi_0, \sin\phi_0)$.

Different terms entering the right-hand side of Eq. (A6) have transparent physical sense. The first term corresponds to ballistic propagation. The second one can be presented as a series over functions P_n (by expanding of the matrix $\hat{M}^{-1}$) which, in fact, is an expansion over number N of collisions (the zero term in this expansion corresponds to $N = 1$) [63]. Having in mind to calculate interference-induced magnetoresistance, we can exclude the term $N = 1$ from the summation [65]. Physically, this term describes return to the initial point after a single scattering, so that corresponding trajectory does not cover any area and, consequently, is not affected by the magnetic field. We neglect both ballistic ($N = 0$) and $N = 1$ terms in the Cooperon propagator, and find

$$C_{\mathbf{Q}}(\phi,\phi_0) = \frac{1}{2\pi(1+\Gamma+i\mathbf{Qn})(1+\Gamma+i\mathbf{Qn}_0)} \times \begin{bmatrix} 1 \\ e^{i(\phi_{\mathbf{Q}}-\phi)} \\ e^{2i(\phi_{\mathbf{Q}}-\phi)}\end{bmatrix}^T \left(\hat{M}^{-1} - \hat{M}^{-1}_{Q=\infty}\right)\begin{bmatrix} 1 \\ e^{i(\phi_0-\phi_{\mathbf{Q}})} \\ e^{2i(\phi_0-\phi_{\mathbf{Q}})}\end{bmatrix}. \tag{A7}$$

Here, we took into account that $P_n \to 0$ for $Q \to \infty$. Let us now find the return probability. To this end, we make expansions

$$\frac{1}{1+\Gamma+i\mathbf{Qn}} = \sum_{n=-\infty}^{\infty} P_n e^{in(\phi-\phi_{\mathbf{Q}})},$$

$$\frac{1}{1+\Gamma+i\mathbf{Qn}_0} = \sum_{m=-\infty}^{\infty} P_m e^{-im(\phi_0-\phi_{\mathbf{Q}})}$$

in Eq. (A7), substitute the obtained equation into Eq. (38), take $\mathbf{r} = \mathbf{r}_0$, and average over $\phi_{\mathbf{Q}}$, thus arriving to Eqs. (40) and (41) of the main text.

2. Nonzero magnetic field

In this Appendix, we find the exact solution of Eq. (50) valid beyond the diffusion approximation. Below, for the sake of brevity, we omit arguments $\mathbf{r}_0$ and ϕ_0 in the Cooperon propagator. First, we make a Fourier transform with respect to x coordinate

$$C(\mathbf{r},\phi) = \int \frac{dk}{2\pi} e^{ikx} C(k,y,\phi) \tag{A8}$$

and rewrite Eq. (50) in a form similar to Eq. (37):

$$C(k,y,\phi) = \hat{R}[C_0(k,y) + e^{-i\phi}C_{-1}(k,y) + e^{-2i\phi}C_{-2}(k,y) + e^{-ikx_0}\delta(y-y_0)\delta(\phi-\phi_0)], \tag{A9}$$

where

$$C_0(k,y) = \frac{1}{1+\eta^2}\int \frac{d\phi}{2\pi} C(k,y,\phi), \tag{A10}$$

$$C_{-1}(k,y) = \frac{2\eta}{1+\eta^2}\int \frac{d\phi}{2\pi} C(k,y,\phi)e^{i\phi}, \tag{A11}$$

$$C_{-2}(k,y) = \frac{\eta^2}{1+\eta^2}\int \frac{d\phi}{2\pi} C(k,y,\phi)e^{2i\phi}, \tag{A12}$$

and

$$\hat{R} = \frac{1}{1+\Gamma+i\hat{\mathbf{q}}\mathbf{n}l} = \frac{1}{1+\Gamma+il\left[\cos\phi\left(k+y/l_B^2\right)+\sin\phi(-i\partial/\partial y)\right]}. \tag{A13}$$

Next, we introduce the canonically conjugated variables

$$\xi_x = l_B\left(k+\frac{y}{l_B^2}\right), \quad \xi_y = -il_B\frac{\partial}{\partial y}, \quad [\hat{\xi}_x,\hat{\xi}_y] = i, \tag{A14}$$

and use the property

$$\boldsymbol{\xi}\mathbf{n} = e^{i\phi a^\dagger a}\xi_x e^{-i\phi a^\dagger a}, \tag{A15}$$

where

$$a^\dagger = \frac{\xi_x - i\xi_y}{\sqrt{2}}, \quad a = \frac{\xi_x + i\xi_y}{\sqrt{2}}, \quad [a,a^\dagger] = 1. \tag{A16}$$

Using this property, we can transform the operator $\hat{R}$ entering the right-hand side of Eq. (A9) as follows:

$$\hat{R} = e^{i\phi a^\dagger a}\frac{1}{1+\Gamma+i\xi_x l/l_B}e^{-i\phi a^\dagger a} \tag{A17}$$

that allows us to present the kernel of this operator in the ξ_x representation in a simple form

$$\langle\xi_x|\hat{R}|\xi_x'\rangle = \sum_{n=0}^{n=\infty}\sum_{m=0}^{m=\infty} e^{i\phi(n-m)}P_{nm}\Psi_n^*(\xi_x)\Psi_m(\xi_x'), \tag{A18}$$

where $\Psi_n(\xi) = \pi^{-1/4}(2^n n!)^{-1/2}\exp(-\xi^2/2)H_n(\xi)$ are the eigenfunction of the harmonic oscillator with the Hamiltonian $a^\dagger a + \frac{1}{2}$ [here, $H_n(\xi)$ are Hermitian polynomials] and

$$P_{nm} = \int_{-\infty}^{\infty} d\xi \frac{\Psi_n^*(\xi)\Psi_m(\xi)}{1+\Gamma+i\xi l/l_B}. \tag{A19}$$

By writing $[1+\Gamma+i\xi l/l_B]^{-1} = (l_B/l)\int_0^\infty dt \exp[-t(1+\Gamma)l_B/l - it\xi]$, after simple calculations we find Eqs. (53) of the main text.

As a next step, we change in Eq. (A9) variable y to ξ_x and expand functions $C(k,y,\phi)$, $C_0(k,y)$, $C_{-1}(k,y,\phi)$, and $C_{-2}(k,y,\phi)$ over a full set of functions $\Psi_n(\xi_x) = \Psi_n(kl_B + y/l_B)$:

$$C(k,y,\phi) = \sum_{n=0}^{\infty} C^{(n)}(k,\phi)\Psi_n(\xi_x), \qquad C_l(k,y) = \sum_{n=0}^{\infty} C_l^{(n)}(k)\Psi_n(\xi_x), \quad l = 0,-1,-2. \tag{A20}$$

Doing so, we find

$$C^{(n)}(k,\phi) = \sum_{m=0}^{\infty} e^{i\phi(n-m)}P_{nm}\left[C_0^{(m)}(k) + e^{-i\phi}C_{-1}^{(m)}(k) + e^{-2i\phi}C_{-2}^{(m)}(k) + l_B^{-1}e^{-ikx_0}\delta(\phi-\phi_0)\Psi_m\left(\xi_x^0\right)\right], \tag{A21}$$

where $\xi_x^0 = kl_B + y_0/l_B$. Now, we multiply Eq. (A21) consequently by 1, $e^{i\phi}$, $e^{2i\phi}$ and average over ϕ having in mind Eqs. (A10)–(A12). Next, we make a replacement $n \to n-1$ and $n \to n-2$ in the second and third of the obtained equations, respectively. As a result, we obtain a system of closed equations for $C_0^{(m)}$, $C_{-1}^{(m-1)}$, and $C_{-2}^{(m-2)}$, the solution of which can be written in a matrix form

$$\begin{bmatrix} C_0^{(m)} \\ C_{-1}^{(m-1)} \\ C_{-2}^{(m-2)} \end{bmatrix} = e^{-ikx_0}\sum_{s=0}^{\infty}\frac{e^{i\phi_0(m-s)}}{2\pi\, l_B}\hat{M}_{m-1}^{-1}\begin{bmatrix} P_{m,s} \\ P_{m-1,s} \\ P_{m-2,s} \end{bmatrix}\Psi_s\left(\xi_x^0\right), \tag{A22}$$

where matrix $\hat{M}_m$ is given by Eq. (52) of the main text and we took into account that $P_{nm} = P_{mn}$. To find the Cooperon propagator, we need to substitute Eq. (A22) into (A21) and then into (A20). Before doing so, we notice that one can extend summation in Eq. (A21) over negative m because by definition $P_{nm} = 0$ for $m < 0$. Neglecting also ballistic contribution described by the term with delta function, we can rewrite Eq. (A21) as

$$C^{(n)}(k,\phi) = \sum_{m=-\infty}^{\infty} e^{i\phi(n-m)}\left[P_{nm}C_0^{(m)}(k) + P_{n,m-1}C_{-1}^{(m-1)}(k) + P_{n,m-2}C_{-2}^{(m-2)}(k)\right]. \tag{A23}$$

Substituting now Eq. (A22) into (A23) and using Eqs. (A8) and (A20), we finally obtain the equation for the Cooperon

propagator in the magnetic field

$$C(\mathbf{r},\mathbf{r}_0,\phi,\phi_0) = \sum_{m=-\infty}^{\infty}\sum_{s=-\infty}^{\infty}\sum_{n=-\infty}^{\infty} \tag{A24}$$

$$\times \int \frac{dk}{2\pi} e^{ik(x-x_0)} \frac{e^{i\phi(n-m)}e^{-i\phi_0(s-m)}}{2\pi\, l_B} \times \begin{bmatrix} P_{nm} \\ P_{n,m-1} \\ P_{n,m-1} \end{bmatrix}^T \left(\hat{M}_{m-1}^{-1} - \hat{M}_{m=\infty}^{-1}\right) \begin{bmatrix} P_{m,s} \\ P_{m-1,s} \\ P_{m-2,s} \end{bmatrix} \times \Psi_s\left(\xi_x^0\right)\Psi_n(\xi_x). \tag{A25}$$

Similar to Eq. (A7), we excluded contribution coming from the processes with a single scattering act. The expression for return probability turns out to be less complicated because for $\mathbf{r} = \mathbf{r}_0$ the integration over k yields

$$\int dk\, \Psi_s(\xi_x)\Psi_n(\xi_x) = \int dk\, \Psi_s(kl_B + y/l_B)\Psi_n(kl_B + y/l_B) = \delta_{n,s} l_B^{-1}, \tag{A26}$$

so that we obtain Eq. (40) where w_n are now given by Eq. (51) of the main text.

APPENDIX B: LIMITING CASES

In this Appendix, we derive Eqs. (69), (70), (72), and (78) directly from Eqs. (41) and (51).

1. Limiting cases for $B = 0$

As we mentioned at the end of Sec. III A for $\eta = 0$ and 1, one of the modes becomes singular. Keeping the singular modes only, one can easily obtain the return probability and the conductivity in vicinities of the points $\eta = 0$ and 1. For $\eta \to 0$, we find from Eq. (41)

$$W(\phi) \approx \frac{w_1}{2\pi l^2}, \quad w_1 \approx \int \frac{d^2\mathbf{Q}}{(2\pi)^2} \frac{P_0^3}{1+\eta^2-P_0}. \tag{B1}$$

Substituting this equation to Eq. (68), we restore with logarithmic precision Eq. (69) of the main text.

For $\eta \to 1$, we find from Eq. (41)

$$W(\phi) \approx \frac{w_0 e^{-i\phi}}{2\pi l^2}, \quad w_0 \approx \int \frac{d^2\mathbf{Q}}{(2\pi)^2} \frac{P_0^3}{1+(1-\eta)^2/2\eta - P_0 - 2P_1^2}. \tag{B2}$$

Again, with logarithmic precision we restore Eq. (70).

2. Limiting cases for $B \neq 0$

Let us calculate magnetoresistance assuming that $\Gamma \ll 1$, $l_B \gg l$, and $\eta \ll 1$ or $1-\eta \ll 1$, respectively. We will start from exact equation (51) valid for $b > 0$ [for $b < 0$ calculations are analogous but one should start from Eq. (82)]. First, we notice that expression for P_{nm} simplifies for $l_B \gg l$. Expanding Eq. (A19) in series over l/l_B and Γ we easily find

$$P_{mm} \approx 1 - \Gamma - b(2m+1), \quad P_{m+1,m} \approx -i\sqrt{b(m+1)} \quad \text{for} \quad m \geq 0, \tag{B3}$$

and $P_{mm} = P_{m+1,m} = 0$ for $m < 0$. Having in mind to invert matrix M_m [see Eq. (52)] we kept linear-in-b terms in P_{mm} which enters diagonal elements of $\hat{M}_m$ and neglected terms higher than $\sqrt{b}$ in the $P_{m+1,m}$ which enters off-diagonal elements. In this approximation, one can neglect $P_{m+2,m}$ which are proportional to b. The ballistic contribution coming from $\hat{M}_{m=\infty}^{-1}$ can be also disregarded.

Next, we find eigenvalues and eigenvectors of $\hat{M}_m$ that allows us diagonalize matrix $\hat{M}_m^{-1}$. Just as in the case $B = 0$, we only keep contributions of the singular modes. One should keep terms of the linear order with respect to b in the eigenvalues, while the eigenvectors can be taken at $b = \Gamma = 0$ and $\eta = 0$ (or $1-\eta = 0$). Results of calculations are presented below separately for $\eta \to 0$ and $1-\eta \to 0$.

(a) $\eta \to 0$. For this case, the singular contribution comes from w_1 that corresponds to zero moment: $M = 0$. Singular eigenvalue of the matrix $\hat{M}_m$ is given by $\lambda_m \approx M_m^{11} - (M_m^{12})^2/M_m^{22} - (M_m^{13})^2/M_m^{33}$. The last two terms in this equation describe mixing of the regular modes with $M = -1$ and -2, respectively, to the singular mode. With the needed precision we get

$$\lambda_m \approx \Gamma + \eta^2 + 2b[m(1+\eta) + 3/2 + \eta]. \tag{B4}$$

In the diffusion approximation, we only keep the singular contribution to the $\hat{M}_m^{-1}$:

$$\hat{M}_m^{-1} \approx \frac{1}{\lambda_m} \begin{bmatrix} 1 & 0 & 0 \\ 0 & 0 & 0 \\ 0 & 0 & 0 \end{bmatrix}. \tag{B5}$$

From Eq. (68) we find that for $\eta \to 0$ the conductivity correction reads as $\delta\sigma = -(e^2/\pi\hbar)[w_1 + w_0/2 + w_2/2]$. The main contribution comes from w_1 which is given by $w_1 \approx (b/\pi)\sum_{m=-\infty}^{\infty} P_{m+1,m+1}^2/\lambda_m \approx (b/\pi)\sum_{n=0}^{\infty} 1/\lambda_{n-1} = (b/\pi)\sum_{n=0}^{\infty} 1/\{\Gamma + \eta^2 + 2b[n(1+\eta) + 1/2]\}$ (here we took into account that $P_{m+1,m+1} = 0$ for $m < -1$ and put $P_{m+1,m+1} \approx 1$ for $m \geqslant 1$). Multiplying both numerator and denominator of the latter equation by $(1+\eta)^{-1} \approx 1-\eta$, and neglecting terms on the order of η^3, $b\eta^2$, and $\Gamma\eta$ in the denominator and terms on the order of $b\eta$ in the numerator, we obtain Eq. (72) of the main text.

(b) $\eta \to 1$. For this case, the singular contribution comes from w_0 that corresponds to $M = -1$. Singular eigenvalue of the matrix $\hat{M}_m$ is given by $\lambda_m \approx M_m^{22} - (M_m^{21})^2/M_m^{11} - (M_m^{23})^2/M_m^{33}$. The last two terms in this equation describe mixing of the regular modes with $M = 0$ and -2, respectively, to the singular mode. With the needed precision we get

$$\lambda_m \approx \Gamma + (1-\eta)^2/2 + 4b[m + 1/2 + (1-\eta)/2]. \tag{B6}$$

In the diffusion approximation, we only keep the singular contribution to the $\hat{M}_m^{-1}$:

$$\hat{M}_m^{-1} \approx \frac{1}{\lambda_m} \begin{bmatrix} 0 & 0 & 0 \\ 0 & -1 & 0 \\ 0 & 0 & 0 \end{bmatrix}. \tag{B7}$$

From these equations we find

$$w_0 = \frac{b}{\pi}\sum_{m=-\infty}^{\infty}\frac{P_{m,m}^2}{\Gamma+(1-\eta)^2/2+4b[m+1/2+(1-\eta)/2]} \approx \frac{b}{\pi}\sum_{m=0}^{N}\frac{1}{\Gamma+(1-\eta)^2/2+4b[m+1/2+(1-\eta)/2]}. \tag{B8}$$

One can see that for $b>0$, Eq. (B8) coincides with Eq. (78) of the main text.

APPENDIX C: KINETIC EQUATION FOR THE COOPERON IN THE PRESENCE OF THE BLOCK MIXING

1. Derivation of the kinetic equation

In the basis (102) matrix elements of the random potential are given by

$$\begin{aligned}\langle 1_{\mathbf{k}}|\hat{V}|1_{\mathbf{k}'}\rangle &= V_{\mathbf{k}\mathbf{k}'}\frac{1+e^{i(\phi'-\phi)}}{1+\eta}\left(\frac{1+\eta}{2}+\Delta\sqrt{\eta}\right),\\ \langle 2_{\mathbf{k}}|\hat{V}|2_{\mathbf{k}'}\rangle &= V_{\mathbf{k}\mathbf{k}'}\frac{1+e^{i(\phi'-\phi)}}{1+\eta}\left(\frac{1+\eta}{2}-\Delta\sqrt{\eta}\right),\\ \langle 1_{\mathbf{k}}|\hat{V}|2_{\mathbf{k}'}\rangle &= \langle 2_{\mathbf{k}}|\hat{V}|1_{\mathbf{k}'}\rangle = V_{\mathbf{k}\mathbf{k}'}\frac{1-e^{i(\phi'-\phi)}}{1+\eta}\left(\frac{1-\eta}{2}\right).\end{aligned} \tag{C1}$$

The single-particle Green's functions are diagonal in this representation and the diagonal elements G^1 and G^2 read as

$$G^1_{R,A}(E,\mathbf{k}) = \frac{1}{E-E_{\mathbf{k}}\pm i\gamma_1/2}, \qquad G^2_{R,A}(E,\mathbf{k}) = \frac{1}{E-E_{\mathbf{k}}\pm i\gamma_2/2}, \tag{C2}$$

where

$$\gamma_1 = \frac{2\pi}{\hbar}\sum_{\alpha=1,2}\int|\langle 1_{\mathbf{k}}|\hat{V}|\alpha_{\mathbf{k}'}\rangle|^2\delta(E_{\mathbf{k}}-E_{\mathbf{k}'})\frac{d^2\mathbf{k}'}{(2\pi)^2} = \gamma_0\frac{1+\eta^2+2\eta\Delta^2+2\Delta\sqrt{\eta}(1+\eta)}{(1+\eta)^2}, \tag{C3}$$

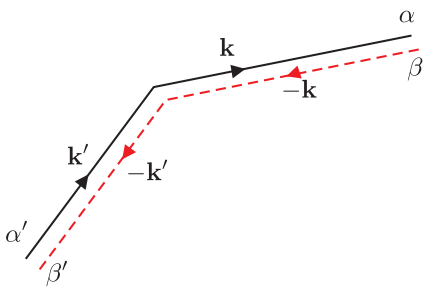

FIG. 20. (Color online) Process corresponding to ingoing term in the collision integral.

$$\gamma_2 = \frac{2\pi}{\hbar}\sum_{\alpha=1,2}\int|\langle 2_{\mathbf{k}}|\hat{V}|\alpha_{\mathbf{k}'}\rangle|^2\delta(E_{\mathbf{k}}-E_{\mathbf{k}'})\frac{d^2\mathbf{k}'}{(2\pi)^2} = \gamma_0\frac{1+\eta^2+2\eta\Delta^2-2\Delta\sqrt{\eta}(1+\eta)}{(1+\eta)^2}. \tag{C4}$$

The Cooperon propagator obeys now the equation which is similar to Eq. (34) but has the matrix form

$$\begin{aligned}&[1/\tau_\phi + i\mathbf{q}\mathbf{v}_F)]C_{\mathbf{q}}^{\alpha\beta,\alpha_0\beta_0}(\phi,\phi_0)\\ &= \int\frac{d\phi'}{2\pi}\gamma_C^{\alpha\beta,\alpha'\beta'}(\phi-\phi')C_{\mathbf{q}}^{\alpha'\beta',\alpha_0\beta_0}(\phi',\phi_0)\\ &\quad-\frac{\gamma_\alpha+\gamma_\beta}{2}C_{\mathbf{q}}^{\alpha\beta,\alpha_0\beta_0}(\phi,\phi_0)+\gamma\delta_{\alpha\alpha_0}\delta_{\beta\beta_0}\delta(\phi-\phi_0).\end{aligned} \tag{C5}$$

Here, we took into account in the outgoing term that the elements of the Cooperon ladder with $\alpha\neq\beta$ decays with the averaged rate $(\gamma_1+\gamma_2)/2$. The ingoing scattering term describes the process shown in Fig. 20. The scattering rate $\gamma_C^{\alpha\beta,\alpha'\beta'}(\phi-\phi')$ is given by Eq. (26) with the replacement $\langle|\tilde{V}_{\mathbf{k}\mathbf{k}'}|^2\rangle$ with $\langle\alpha_{\mathbf{k}}|\hat{V}|\alpha'_{\mathbf{k}'}\rangle\langle\beta_{-\mathbf{k}}|\hat{V}|\beta'_{-\mathbf{k}'}\rangle$ where matrix elements are given by Eq. (C1). The expression for conductivity is given by Eq. (66) with the replacement of $W(\phi)\gamma_C(\pi-\phi)$ with $\sum_{\alpha\beta\alpha'\beta'}W^{\alpha\beta,\alpha'\beta'}(\phi)\gamma_C^{\alpha'\beta',\beta\alpha}(\pi-\phi)$, where $W^{\alpha\beta,\alpha'\beta'}(\phi)$ is found from Eqs. (38) and (39) with the replacement of C with $C^{\alpha\beta,\alpha'\beta'}$(we note that indices α and β enter in different order in $W^{\alpha\beta,\alpha'\beta'}$ and $\gamma_C^{\alpha'\beta',\beta\alpha}$).

Equation (C5) can be rewritten in a more compact way by expanding both Cooperon and scattering rate matrices over the Pauli matrices $\hat{\sigma}_{(n)}$ ($n=0,1,2,3$ and $\hat{\sigma}_0$ is the unit 2×2 matrix):

$$\gamma_C^{\alpha\beta,\alpha'\beta'}(\phi-\phi') = \sigma_{(n)}^{\alpha\beta}\gamma_C^{nm}(\phi-\phi')\sigma_{(m)}^{\beta'\alpha'}/2, \tag{C6}$$

$$C_{\mathbf{q}}^{\alpha\beta,\alpha'\beta'}(\phi,\phi_0) = \sigma_{(n)}^{\alpha\beta}C_{\mathbf{q}}^{nm}(\phi,\phi_0)\sigma_{(m)}^{\beta'\alpha'}/2. \tag{C7}$$

Here, $C_{\mathbf{q}}^{nm}$, γ_C^{nm} are elements of 4×4 matrices. After simple calculations, we arrive to Eqs. (103) and (104) of the main text where

$$\hat{\gamma}_0 = \frac{\gamma_0}{(1+\eta)^2}\begin{bmatrix}(1+\eta^2+2\eta\Delta^2)/2 & (1-\eta^2)/2 & 0 & \Delta\sqrt{\eta}(1+\eta)\\ (1-\eta^2)/2 & (1+\eta^2-2\eta\Delta^2)/2 & 0 & \Delta\sqrt{\eta}(1-\eta)\\ 0 & 0 & \eta(1-\Delta^2) & 0\\ \Delta\sqrt{\eta}(1+\eta) & \Delta\sqrt{\eta}(1-\eta) & 0 & \eta(1+\Delta^2)\end{bmatrix}, \tag{C8}$$

$$\hat{\gamma}_{-1} = \frac{\gamma_0}{(1+\eta)^2}\begin{bmatrix} 2\eta(1+\Delta^2) & 0 & 0 & 2\Delta\sqrt{\eta}(1+\eta) \\ 0 & 2\eta(1-\Delta^2) & 0 & 0 \\ 0 & 0 & 1+\eta^2-2\eta\Delta^2 & 0 \\ 2\Delta\sqrt{\eta}(1+\eta) & 0 & 0 & 1+\eta^2+2\eta\Delta^2 \end{bmatrix}, \tag{C9}$$

$$\hat{\gamma}_{-2} = \frac{\gamma_0}{(1+\eta)^2}\begin{bmatrix} (1+\eta^2+2\eta\Delta^2)/2 & -(1-\eta^2)/2 & 0 & \Delta\sqrt{\eta}(1+\eta) \\ -(1-\eta^2)/2 & (1+\eta^2-2\eta\Delta^2)/2 & 0 & -\Delta\sqrt{\eta}(1-\eta) \\ 0 & 0 & \eta(1-\Delta^2) & 0 \\ \Delta\sqrt{\eta}(1+\eta) & -\Delta\sqrt{\eta}(1-\eta) & 0 & \eta(1+\Delta^2) \end{bmatrix}, \tag{C10}$$

$$\hat{\gamma}_D = \begin{bmatrix} (\gamma_1+\gamma_2)/2 & 0 & 0 & (\gamma_1-\gamma_2)/2 \\ 0 & (\gamma_1+\gamma_2)/2 & 0 & 0 \\ 0 & 0 & (\gamma_1+\gamma_2)/2 & 0 \\ (\gamma_1-\gamma_2)/2 & 0 & 0 & (\gamma_1+\gamma_2)/2 \end{bmatrix} \tag{C11}$$

$$= \frac{\gamma_0}{(1+\eta)^2}\begin{bmatrix} 1+\eta^2+2\eta\Delta^2 & 0 & 0 & 2\Delta\sqrt{\eta}(1+\eta) \\ 0 & 1+\eta^2+2\eta\Delta^2 & 0 & 0 \\ 0 & 0 & 1+\eta^2+2\eta\Delta^2 & 0 \\ \Delta\sqrt{\eta}(1+\eta) & 0 & 0 & 1+\eta^2+2\eta\Delta^2 \end{bmatrix}. \tag{C12}$$

2. Matrices entering expression for the conductivity corrections

From Eqs. (C8), (C10), (C9), and (107), we find matrices entering Eq. (109). For our purposes, it is sufficient to know these matrices for $\Delta = 0$:

$$\frac{\hat{\gamma}_{-2}\hat{\xi}}{2} = \frac{\gamma_0}{(1+\eta)^2}\begin{bmatrix} \frac{1+\eta^2}{4} & -\frac{1-\eta^2}{4} & 0 & 0 \\ -\frac{1-\eta^2}{4} & \frac{1+\eta^2}{4} & 0 & 0 \\ 0 & 0 & -\frac{\eta}{2} & 0 \\ 0 & 0 & 0 & \frac{\eta}{2} \end{bmatrix}, \tag{C13}$$

$$\frac{\hat{\gamma}_{0}\hat{\xi}}{2} = \frac{\gamma_0}{(1+\eta)^2}\begin{bmatrix} \frac{1+\eta^2}{4} & \frac{1-\eta^2}{4} & 0 & 0 \\ \frac{1-\eta^2}{4} & \frac{1+\eta^2}{4} & 0 & 0 \\ 0 & 0 & -\frac{\eta}{2} & 0 \\ 0 & 0 & 0 & \frac{\eta}{2} \end{bmatrix}, \tag{C14}$$

$$\left(\hat{\gamma}_{-2} - \frac{\hat{\gamma}_{-1}}{2}\right)\hat{\xi} = \frac{\gamma_0}{(1+\eta)^2}\begin{bmatrix} \frac{(1-\eta)^2}{2} & -\frac{1-\eta^2}{2} & 0 & 0 \\ -\frac{1-\eta^2}{2} & \frac{(1-\eta)^2}{2} & 0 & 0 \\ 0 & 0 & \frac{(1-\eta)^2}{2} & 0 \\ 0 & 0 & 0 & -\frac{(1-\eta)^2}{2} \end{bmatrix}, \tag{C15}$$

$$\left(\hat{\gamma}_{0} - \frac{\hat{\gamma}_{-1}}{2}\right)\hat{\xi} = \frac{\gamma_0}{(1+\eta)^2}\begin{bmatrix} \frac{(1-\eta)^2}{2} & \frac{1-\eta^2}{2} & 0 & 0 \\ \frac{1-\eta^2}{2} & \frac{(1-\eta)^2}{2} & 0 & 0 \\ 0 & 0 & \frac{(1-\eta)^2}{2} & 0 \\ 0 & 0 & 0 & -\frac{(1-\eta)^2}{2} \end{bmatrix}, \tag{C16}$$

$$\left(\hat{\gamma}_{-1} - \frac{\hat{\gamma}_{0}+\hat{\gamma}_{-2}}{2}\right)\hat{\xi} = \frac{\gamma_0}{(1+\eta)^2}\begin{bmatrix} 2\eta - \frac{1+\eta^2}{2} & 0 & 0 & 0 \\ 0 & 2\eta - \frac{1+\eta^2}{2} & 0 & 0 \\ 0 & 0 & \eta-1-\eta^2 & 0 \\ 0 & 0 & 0 & 1+\eta^2-\eta \end{bmatrix}. \tag{C17}$$

3. Matrices determining gaps of the diffusive modes

From Eqs. (C8), (C10), (C9), and (C11), we found matrices whose eigenvalues yield gaps of the diffusive Cooperon modes:

$$\hat{\gamma}_D - \hat{\gamma}_0 = \frac{\gamma_0}{(1+\eta)^2}\begin{bmatrix} \frac{1+\eta^2+2\eta\Delta^2}{2} & -\frac{1-\eta^2}{2} & 0 & \Delta\sqrt{\eta}(1+\eta) \\ -\frac{1-\eta^2}{2} & \frac{1+\eta^2+6\eta\Delta^2}{2} & 0 & -\Delta\sqrt{\eta}(1-\eta) \\ 0 & 0 & 1+\eta^2-\eta+3\eta\Delta^2 & 0 \\ \Delta\sqrt{\eta}(1+\eta) & -\Delta\sqrt{\eta}(1-\eta) & 0 & 1+\eta^2-\eta+\eta\Delta^2 \end{bmatrix}, \tag{C18}$$

$$\hat{\gamma}_D - \hat{\gamma}_{-2} = \frac{\gamma_0}{(1+\eta)^2}\begin{bmatrix} \frac{1+\eta^2+2\eta\Delta^2}{2} & \frac{1-\eta^2}{2} & 0 & \Delta\sqrt{\eta}(1+\eta) \\ \frac{1-\eta^2}{2} & \frac{1+\eta^2+6\eta\Delta^2}{2} & 0 & \Delta\sqrt{\eta}(1-\eta) \\ 0 & 0 & 1+\eta^2-\eta+3\eta\Delta^2 & 0 \\ \Delta\sqrt{\eta}(1+\eta) & \Delta\sqrt{\eta}(1-\eta) & 0 & 1+\eta^2-\eta+\eta\Delta^2 \end{bmatrix}, \tag{C19}$$

$$\hat{\gamma}_D - \hat{\gamma}_{-1} = \frac{\gamma_0}{(1+\eta)^2}\begin{bmatrix} (1-\eta)^2 & 0 & 0 & 0 \\ 0 & (1-\eta)^2+4\eta\Delta^2 & 0 & 0 \\ 0 & 0 & 4\eta\Delta^2 & 0 \\ 0 & 0 & 0 & 0 \end{bmatrix}. \tag{C20}$$

We see that matrix $\hat{\gamma}_D - \hat{\gamma}_{-1}$ has two eigenvalues which turn to zero at $\Delta = 0$. As shown in the main text, two corresponding diffusive modes cancel each other in the limit $\Delta \to 0$.

4. Generalization of the diffusion approximation for the case of block mixing

In this Appendix, we generalize the diffusion approximation for the case of the block mixing. This approximation is valid for $ql \ll 1$, when the coupling of different harmonics is weak and the mode $e^{iM\phi}$ is only effectively coupled with the nearest modes $e^{i(M\pm1)\phi}$. In a full analogy with Sec. III C, we find from Eqs. (103), (104), (106), and (108)

$$\hat{w}_{M+1} = \int \frac{\gamma}{\gamma_\varphi + \hat{\gamma}_D - \hat{\gamma}_M + q^2\hat{D}_M}\frac{l^2d^2\mathbf{q}}{(2\pi)^2}. \tag{C21}$$

Here, operator $q^2\hat{D}_M$ in the denominator of the integrand appeared due to the coupling with $M \pm 1$ modes:

$$q^2\hat{D}_M = v_F^2\left\langle \mathbf{qn}\frac{1}{\gamma_\varphi - \hat{\gamma}_D - \hat{\gamma}_C}\mathbf{qn}\right\rangle_M = \frac{q^2v_F^2}{4}(\hat{\tau}_{M+1} + \hat{\tau}_{M-1}), \tag{C22}$$

where $\hat{\gamma}_C$ is the operator with the matrix kernel given by Eq. (104), $\langle \ldots \rangle_M$ stands for projection on the mode $\exp(iM\phi)$,

$$\hat{\tau}_M = \frac{1}{\gamma_\varphi + \hat{\gamma}_D - \hat{\gamma}_M} \approx \frac{1}{\hat{\gamma}_D - \hat{\gamma}_M}, \tag{C23}$$

and $\hat{\gamma}_M$ is given by Eqs. (C8)–(C10) for $M = 0, -1, -2$, respectively ($\gamma_M = 0$ for other values of M). Hence,

$$\hat{D}_M = \frac{v_F^2(\hat{\tau}_{M+1} + \hat{\tau}_{M-1})}{4}. \tag{C24}$$

For convenience, the matrices $\hat{w}_n$ entering Eq. (109) are presented as follows:

$$\hat{w}_{-2} = \int \frac{\gamma}{\gamma_\varphi + \hat{\gamma}_D + q^2\hat{D}_{-3}}\frac{l^2d^2\mathbf{q}}{(2\pi)^2}, \tag{C25}$$

$$\hat{w}_{-1} = \int \frac{\gamma}{\gamma_\varphi + \hat{\gamma}_D - \hat{\gamma}_{-2} + q^2\hat{D}_{-2}}\frac{l^2d^2\mathbf{q}}{(2\pi)^2}, \tag{C26}$$

$$\hat{w}_0 = \int \frac{\gamma}{\gamma_\varphi + \hat{\gamma}_D - \hat{\gamma}_{-1} + q^2\hat{D}_{-1}}\frac{l^2d^2\mathbf{q}}{(2\pi)^2}, \tag{C27}$$

$$\hat{w}_1 = \int \frac{\gamma}{\gamma_\varphi + \hat{\gamma}_D - \hat{\gamma}_0 + q^2\hat{D}_0}\frac{l^2d^2\mathbf{q}}{(2\pi)^2}, \tag{C28}$$

$$\hat{w}_2 = \int \frac{\gamma}{\gamma_\varphi + \hat{\gamma}_D + q^2\hat{D}_1}\frac{l^2d^2\mathbf{q}}{(2\pi)^2}, \tag{C29}$$

where

$$\hat{D}_{-3} = \frac{v_F^2(\tau_{-2}+\tau_{-4})}{4} = \frac{v_F^2}{4}\left(\frac{1}{\hat{\gamma}_D - \hat{\gamma}_{-2}} + \frac{1}{\hat{\gamma}_D}\right), \tag{C30}$$

$$\hat{D}_{-2} = \frac{v_F^2(\tau_{-1}+\tau_{-3})}{4} = \frac{v_F^2}{4}\left(\frac{1}{\hat{\gamma}_D - \hat{\gamma}_{-1}} + \frac{1}{\hat{\gamma}_D}\right), \tag{C31}$$

$$\hat{D}_{-1} = \frac{v_F^2(\tau_0+\tau_{-2})}{4} = \frac{v_F^2}{4}\left(\frac{1}{\hat{\gamma}_D - \hat{\gamma}_0} + \frac{1}{\hat{\gamma}_D - \hat{\gamma}_{-2}}\right), \tag{C32}$$

$$\hat{D}_0 = \frac{v_F^2(\tau_1+\tau_{-1})}{4} = \frac{v_F^2}{4}\left(\frac{1}{\hat{\gamma}_D} + \frac{1}{\hat{\gamma}_D - \hat{\gamma}_{-1}}\right), \tag{C33}$$

$$\hat{D}_1 = \frac{v_F^2(\tau_2+\tau_0)}{4} = \frac{v_F^2}{4}\left(\frac{1}{\hat{\gamma}_D} + \frac{1}{\hat{\gamma}_D - \hat{\gamma}_0}\right). \tag{C34}$$

The results obtained above in this section can be easily generalized for the case of weak magnetic field such that

dimensionless field b is much smaller that unity. To this end, one should slightly modify Eq. (C22) taking into account that for $b \neq 0$ operators $\hat{q}_x$ and $\hat{q}_y$ no longer commute. Simple calculation yields

$$v_F^2 \left(\mathbf{qn}\frac{1}{\gamma_\varphi - \hat{\gamma}_D - \hat{\gamma}_C}\mathbf{qn}\right)_M = \frac{(\hat{q}_x^2+\hat{q}_y^2)v_F^2}{4}(\hat{\tau}_{M+1}+\hat{\tau}_{M-1}) + \frac{i[\hat{q}_x,\hat{q}_y]v_F^2}{4}(\hat{\tau}_{M-1}-\hat{\tau}_{M+1}). \quad \text{(C35)}$$

Replacing operator $\hat{q}_x^2+\hat{q}_y^2$ by its eigenvalue $(4/l^2)|b|(n+1/2)$, we find that one should make the following replacement in Eq. (C21):

$$q^2\hat{D}_M \to \gamma^2\left[|b|\left(n+\frac{1}{2}\right)(\hat{\tau}_{M+1}+\hat{\tau}_{M-1}) - b\frac{\hat{\tau}_{M-1}-\hat{\tau}_{M+1}}{2}\right] \quad \text{(C36)}$$

and also replace integral over $l^2d^2\mathbf{q}/(2\pi)^2$ with the $(|b|/\pi)\sum_{n=0}^{N\sim 1/|b|}$.

While substituting $\hat{\tau}_{M\pm1}$ into this equation one can set $\Delta = 0$. Corresponding sums can be calculated with the use of Eq. (75).

APPENDIX D: CALCULATION OF CONDUCTIVITY CORRECTION IN THE PRESENCE OF THE BLOCK MIXING

In this Appendix, we present calculation of conductivity correction in the presence of the block mixing.

1. $B = 0$

Let us start with calculation of the contributions of ISM. These modes correspond to two eigenvalues (elements 33 and 44 of the diagonal matrix $\hat{\gamma}_D - \hat{\gamma}_{-1}$), one of which equals to zero at any Δ and another one turns to zero at $\Delta \to 0$. These modes give contribution to conductivity $\delta\sigma_{\rm ISM}$, which comes from w_0 :

$$\delta\sigma_{\rm ISM} \approx \frac{e^2}{2\pi\hbar}\left(\frac{l_{tr}}{l}\right)^2\frac{1}{\gamma}\mathrm{Tr}\left[\left(\hat{\gamma}_{-1}-\frac{\hat{\gamma}_0+\hat{\gamma}_{-2}}{2}\right)\hat{\xi}\hat{w}_0\right] = \frac{e^2}{2\pi\hbar}\int\frac{l_{tr}^2d^2\mathbf{q}}{(2\pi)^2}\mathrm{Tr}\left[\left(\hat{\gamma}_{-1}-\frac{\hat{\gamma}_0+\hat{\gamma}_{-2}}{2}\right)\times\hat{\xi}\frac{1}{\gamma_\varphi+\hat{\gamma}_D-\hat{\gamma}_{-1}+q^2\hat{D}_{-1}}\right]. \quad \text{(D1)}$$

Further calculations will be performed within the diffusion approximation, which was generalized for the case of the block mixing in Appendix C 4. First, we project matrices $\hat{\gamma}_D - \hat{\gamma}_{-1}$, $[\hat{\gamma}_{-1}-(\hat{\gamma}_0+\hat{\gamma}_{-2})/2]\hat{\xi}$, and $\hat{D}_{-1}$ on the space formed by eigenvectors corresponding to ISM (this means that we take in these 4×4 matrices their bottom-right 2×2 blocks). From Eqs. (C17), (C32), (C18), and (C19) we find projected matrices (in all these matrices except $\hat{\gamma}_D-\hat{\gamma}_{-1}$ one can approximately set $\Delta = 0$)

$$\hat{\gamma}_D-\hat{\gamma}_{-1} \to \frac{\gamma_0}{(1+\eta)^2}\begin{bmatrix}4\eta\Delta^2 & 0\\ 0 & 0\end{bmatrix}, \quad \text{(D2)}$$

$$\left(\hat{\gamma}_{-1}-\frac{\hat{\gamma}_0+\hat{\gamma}_{-2}}{2}\right)\hat{\xi} \to \gamma_0\frac{1+\eta^2-\eta}{(1+\eta)^2}\begin{bmatrix}-1 & 0\\ 0 & 1\end{bmatrix}, \quad \text{(D3)}$$

$$\hat{D}_{-1} \to \frac{v_F^2}{2\gamma_0}\frac{(1+\eta)^2}{1+\eta^2-\eta}\begin{bmatrix}1 & 0\\ 0 & 1\end{bmatrix}. \quad \text{(D4)}$$

Substituting these projected matrices into Eq. (D1), neglecting Δ everywhere except gap of one of the singular modes, after simple calculations we find for contribution of ISM Eq. (110) of the main text.

Next, we discuss special points $\eta = 0$ and 1. We start from the case $\eta \approx 1$. Above, we projected all matrices entering Eq. (D1) on the basis formed by eigenvectors corresponding to smallest eigenvalues of the matrix $\hat{\gamma}_D-\hat{\gamma}_{-1}$. Such an approximation works well only far from the point $\eta = 1$. Indeed, as seen from Eq. (C20) for η close to 1, two other eigenvalues of the matrix $\hat{\gamma}_D-\hat{\gamma}_{-1}$ (matrix elements 11 and 22 of this diagonal matrix) become small and contribution of two corresponding modes come into play. Let us now project the matrices $\hat{\gamma}_D-\hat{\gamma}_{-1}$, $[\hat{\gamma}_{-1}-(\hat{\gamma}_0+\hat{\gamma}_{-2})/2]\hat{\xi}$, and $\hat{D}_{-1}$ on the space formed by these eigenvectors. From Eqs. (C17), (C32), (C18), and (C19) we find

$$\hat{\gamma}_D-\hat{\gamma}_{-1} \to \frac{\gamma_0}{(1+\eta)^2}\begin{bmatrix}(1-\eta)^2 & 0\\ 0 & (1-\eta)^2+4\Delta^2\eta\end{bmatrix} \approx \frac{\gamma_0}{4}\begin{bmatrix}(1-\eta)^2 & 0\\ 0 & (1-\eta)^2+4\Delta^2\end{bmatrix}, \quad \text{(D5)}$$

$$\left(\hat{\gamma}_{-1}-\frac{\hat{\gamma}_0+\hat{\gamma}_{-2}}{2}\right)\hat{\xi} \to \frac{\gamma_0}{(1+\eta)^2}\left(2\eta-\frac{1+\eta^2}{2}\right)\begin{bmatrix}1 & 0\\ 0 & 1\end{bmatrix} \approx \frac{\gamma_0}{4}\begin{bmatrix}1 & 0\\ 0 & 1\end{bmatrix}, \quad \text{(D6)}$$

$$\hat{D}_{-1} \to \frac{v_F^2(1+\eta)^2(1+\eta^2)}{4\gamma_0\eta^2}\begin{bmatrix}1 & 0\\ 0 & 1\end{bmatrix} \approx \frac{2v_F^2}{\gamma_0}\begin{bmatrix}1 & 0\\ 0 & 1\end{bmatrix}. \quad \text{(D7)}$$

Substituting these projected matrices into Eq. (D1), neglecting Δ everywhere except gap of one of the diffusive modes, after simple calculations we find contribution $\delta\sigma_{1-\eta}$ given by Eq. (123) of the main text.

Now, we turn to the case $\eta \to 0$. Analyzing Eqs. (C25)–(C29), one can see that for $\eta \ll 1$ contributions to conductivity coming from matrices $\hat{w}_{-1}$ and $\hat{w}_1$ should be taken into account because matrices $\hat{\gamma}_D - \hat{\gamma}_0$ and $\hat{\gamma}_D - \hat{\gamma}_{-2}$ have zero eigenvalues in the limit $\eta \to 0$ and $\Delta \to 0$. Let us consider the corresponding contribution to the conductivity:

$$\delta\sigma_\eta \approx \frac{e^2}{2\pi\hbar}\left(\frac{l_{tr}}{l}\right)^2 \frac{1}{\gamma}\mathrm{Tr}\left[\left(\hat{\gamma}_{-2} - \frac{\hat{\gamma}_{-1}}{2}\right)\hat{\xi}\,\hat{w}_{-1} + \left(\hat{\gamma}_0 - \frac{\hat{\gamma}_{-1}}{2}\right)\hat{\xi}\,\hat{w}_1\right]$$
$$= \frac{e^2}{2\pi\hbar}\int \frac{l_{tr}^2 d^2\mathbf{q}}{(2\pi)^2}\mathrm{Tr}\left[\left(\hat{\gamma}_{-2} - \frac{\hat{\gamma}_{-1}}{2}\right)\hat{\xi}\,\frac{1}{\gamma_\varphi + \hat{\gamma}_D - \hat{\gamma}_{-2} + q^2\hat{D}_{-2}} + \left(\hat{\gamma}_0 - \frac{\hat{\gamma}_{-1}}{2}\right)\hat{\xi}\,\frac{1}{\gamma_\varphi + \hat{\gamma}_D - \hat{\gamma}_0 + q^2\hat{D}_0}\right]. \quad \text{(D8)}$$

The two terms in the square brackets represent contributions of two blocks, respectively.

From Eqs. (C18) and (C19), we see that after neglecting terms proportional to Δ in the off-diagonal elements of matrices $\hat{\gamma}_D - \hat{\gamma}_0$ and $\hat{\gamma}_D - \hat{\gamma}_{-2}$ these matrices become block matrices consisting of left-upper and right-bottom 2×2 blocks. For both matrices, small eigenvalues (for small η and Δ) correspond to the left-upper block. Projecting all matrices entering Eq. (D8) on this block, we then transform projected matrices by unitary transformation

$$\hat{U} = \frac{1}{\sqrt{2}}\begin{bmatrix}1 & -1\\ 1 & 1\end{bmatrix}. \quad \text{(D9)}$$

After this transformation, off-diagonal elements of all projected matrices become small and can be neglected. One can also neglect η and Δ in diagonal elements which remain finite at $\eta \to 0$ and $\Delta \to 0$. Then, we obtain

$$\hat{U}(\hat{\gamma}_D - \hat{\gamma}_0)\hat{U}^{-1} \to \gamma_0\begin{bmatrix}1 & 0\\ 0 & \eta^2 + 2\eta\Delta^2\end{bmatrix}, \quad \text{(D10)}$$

$$\hat{U}(\hat{\gamma}_D - \hat{\gamma}_{-2})\hat{U}^{-1} \to \gamma_0\begin{bmatrix}\eta^2 + 2\eta\Delta^2 & 0\\ 0 & 1\end{bmatrix}, \quad \text{(D11)}$$

$$\hat{U}\left(\hat{\gamma}_{-2} - \frac{\hat{\gamma}_{-1}}{2}\right)\hat{\xi}\,\hat{U}^{-1} \to \gamma_0\begin{bmatrix}1 & 0\\ 0 & 0\end{bmatrix}, \quad \text{(D12)}$$

$$\hat{U}\left(\hat{\gamma}_0 - \frac{\hat{\gamma}_{-1}}{2}\right)\hat{\xi}\,\hat{U}^{-1} \to \gamma_0\begin{bmatrix}0 & 0\\ 0 & 1\end{bmatrix}, \quad \text{(D13)}$$

$$\hat{D}_{-2} = \hat{D}_0 \to \frac{v_F^2}{2\gamma_0}\begin{bmatrix}1 & 0\\ 0 & 1\end{bmatrix}. \quad \text{(D14)}$$

After some simple algebra, we arrive to Eq. (118) of the main text.

2. $B \neq 0$

The results obtained in Appendix C 4 can be also used for calculation of the conductivity correction in weak magnetic field ($b \ll 1$). First, we calculate $\delta\sigma_{\mathrm{ISM}}(b) - \delta\sigma_{\mathrm{ISM}}(0)$. In this case, $M = -1$ and projection of the matrix $\hat{\tau}_{-2} - \hat{\tau}_0$ at the block corresponding to ISM goes to zero for $\Delta \to 0$. Hence, the only effect of the magnetic field is the replacement everywhere of the integration over $d^2\mathbf{q}$ with the summation over n. Simple calculations yield Eq. (112) of the main text.

Calculation of $\Delta\sigma_{1-\eta} = \delta\sigma_{1-\eta}(b) - \delta\sigma_{1-\eta}(0)$ is more tricky. In this case, projection of $\hat{\tau}_{-2} - \hat{\tau}_0$ to the upper-left block is approximately given by

$$\hat{\tau}_{-2} - \hat{\tau}_0 \to -\frac{8(1-\eta)}{\gamma_0}\begin{bmatrix}0 & 1\\ 1 & 0\end{bmatrix}$$

and does not commute with the projection of the matrix $\hat{\gamma}_D - \hat{\gamma}_{-1}$ on the upper-left block which is approximately given by

$$\hat{\gamma}_D - \hat{\gamma}_{-1} \to \frac{\gamma_0}{4}\begin{bmatrix}(1-\eta)^2 & 0\\ 0 & (1-\eta)^2 + 4\eta\Delta^2\end{bmatrix}$$

(this matrix determines the diffusive gaps in this channel). Calculations can be performed by using simple generalization of Eq. (75) to the matrix case:

$$\mathrm{Tr}\left[\sum_{n=0}^{n=N}\frac{b}{b(n+1/2) + \hat{A}}\right] \quad \text{(D15)}$$
$$= 2\ln N - \psi(A_1/b + 1/2) - \psi(A_2/b + 1/2)$$
$$\approx \begin{cases}2\ln\left(\frac{1}{b}\right), & b \gg A_1, A_2\\ \ln\left(\frac{1}{\det\hat{A}}\right) - \frac{b^2}{24}\left(\frac{1}{A_1^2} + \frac{1}{A_2^2}\right), & b \ll A_1, A_2\end{cases} \quad \text{(D16)}$$

where $A_{1,2}$ are eigenvalues of matrix $\hat{A}$. Using Eq. (D15), after some algebra we find Eq. (126) of the main text.

Finally, we calculate $\Delta\sigma_\eta = \delta\sigma_\eta(b) - \delta\sigma_\eta(0)$. In this case, additional matrices arising in the denominators of Eqs. (C26) and (C28) due to noncommutativity of $\hat{q}_x$ and $\hat{q}_y$ are proportional to unit matrix, so that calculations are quite analogous to the calculations of $\Delta\sigma_{\mathrm{ISM}}$. The result is given by Eq. (121) of the main text.

APPENDIX E: STRONG-FIELD ASYMPTOTIC

For strong B, such that $l_B/l \ll 1$, the expression for the conductivity correction simplifies. First of all, from Eq. (A19) we find in this limit

$$P_{nm} = \frac{l_B}{l}\int_{-\infty}^{\infty} d\xi\,\frac{\Psi_n^*(\xi)\Psi_m(\xi)}{(1+\Gamma)(l_B/l) + i\xi}$$
$$\approx -\frac{il_B}{l}\int_{-\infty}^{\infty} d\xi\,\frac{\Psi_n^*(\xi)\Psi_m(\xi)}{\xi - i0}. \quad \text{(E1)}$$

Hence, P_{nm} decreases as a square root of the field $P_{nm} \propto 1/\sqrt{b}$ and becomes small $P_{nm} \ll 1$ at sufficiently large b. Therefore, one can expand matrices $\hat{M}_m^{-1} - \hat{M}_{m=\infty}^{-1}$ entering Eqs. (51) and (82) in the series over P_{nm} and keep the terms of the

lowest order only. Doing so, we find

$$w_n(b\to\infty) = \frac{l^2}{2\pi l_B^2}\frac{1}{(1+\eta^2)^2}\sum_{m=-\infty}^{m=\infty}\big[P^2_{n+m,m+1}P_{m+1,m+1} + 4\eta P_{n+m,m+1}P_{m+1,m}P_{n+m,m} + 2\eta^2\big(P_{n+m,m-1}P_{m+1,m-1}P_{n+m,m+1} + 2P^2_{n+m,m}P_{m,m}\big) + 4\eta^3 P_{n+m,m}P_{m,m-1}P_{n+m,m-1} + \eta^4 P^2_{n+m,m-1}P_{m-1,m-1}\big], \tag{E2}$$

$$w_n(b\to-\infty) = \frac{l^2}{2\pi l_B^2}\frac{1}{(1+\eta^2)^2}\sum_{m=-\infty}^{m=\infty}\big[P^2_{m-n,m-1}P_{m-1,m-1} + 4\eta P_{m-n,m-1}P_{m-1,m}P_{m-n,m} + 2\eta^2\big(P_{m-n,m+1}P_{m+1,m-1}P_{m-n,m-1} + 2P^2_{m-n,m}P_{m,m}\big) + 4\eta^3 P_{m-n,m}P_{m,m+1}P_{m-n,m+1} + \eta^4 P^2_{m-n,m+1}P_{m+1,m+1}\big]. \tag{E3}$$

For calculation of the conductivity, we need to know w_n for $n=-2,-1,0,1,2$. Therefore, for our purposes it is sufficient to find $P_{n,m}$ with $|n-m|\le 3$. From Eq. (E2) one can find

$$P_{2k,2k} = \frac{l_B}{l}\frac{\sqrt{\pi}}{2^{2k}}\frac{(2k)!}{(k!)^2}\theta(k),$$

$$P_{2k+1,2k} = P_{2k,2k+1} = -\frac{il_B}{l}\frac{\sqrt{2}}{\sqrt{2k+1}}\theta(k),$$

$$P_{2k+2,2k} = P_{2k,2k+2} = -\frac{l_B}{l}\frac{\sqrt{\pi}}{2^{2k+1}}\frac{\sqrt{(2k)!(2k+2)!}}{k!(k+1)!}\theta(k), \tag{E4}$$

$$P_{2k+3,2k} = P_{2k,2k+3} = \frac{il_B}{l}\frac{\sqrt{8}(k+1)}{\sqrt{(2k+1)(2k+2)(2k+3)}}\theta(k),$$

where $\theta(k)$ is the step function defined such that $\theta(k)=1$ for $k\geqslant 0$ and $\theta(k)=0$ for negative k.

Using Eqs. (E2)–(E4), after cumbersome but straightforward calculations we find Eq. (127) of the main text, where the coefficient $A_{\rm II}(\eta)$ is different for the positive and negative b:

$$A_{{\rm II},b\to\infty}(\eta) = \frac{\sqrt{\pi}}{4}\frac{1}{(1+\eta^2)(1-\eta+\eta^2)^2}\left[1+4\eta-7\eta^2-2\eta^3-\frac{25\eta^4}{4}+4\eta^5+\eta^6 - \frac{\pi(2-3\eta+9\eta^2-20\eta^3+9\eta^4-3\eta^5+2\eta^6)}{\Gamma^4(3/4)} + \frac{4\eta(-1+\eta-\eta^3+\eta^4)\Gamma^4(3/4)}{\pi^3}\right], \tag{E5}$$

$$A_{{\rm II},b\to-\infty}(\eta) = \frac{\sqrt{\pi}}{4}\frac{1}{(1+\eta^2)(1-\eta+\eta^2)^2}\left[1+4\eta-\frac{25\eta^2}{4}-2\eta^3-7\eta^4+4\eta^5+\eta^6 - \frac{\pi(2-3\eta+9\eta^2-20\eta^3+9\eta^4-3\eta^5+2\eta^6)}{\Gamma^4(3/4)} - \frac{4\eta(-1+\eta-\eta^3+\eta^4)\Gamma^4(3/4)}{\pi^3}\right]. \tag{E6}$$

Here, $\Gamma(x)$ is the gamma function.

The strong-field asymptotics of the magnetoconductivity calculated in this appendix reflects the statistics of areas and Berry phases for minimal (triangular) trajectories contributing to the conductivity correction. The analytical expression for $\eta=0$,

$$A_{{\rm II},b\to\infty}(0) = A_{{\rm II},b\to-\infty}(0) = \frac{\sqrt{\pi}}{4}\left[1-\frac{2\pi}{\Gamma^4(3/4)}\right], \tag{E7}$$

reproduces the numerical prefactor found for the weak localization in a parabolic band in the absence of the Berry phase in Refs. [59,60]:

$$A_{{\rm I},b\to\infty}(0) + A_{{\rm II},b\to\infty}(0) = 2A_{{\rm II},b\to\infty}(0) \simeq -\frac{4.974}{\pi}.$$

[1] L. P. Gorkov, A. I. Larkin, and D. E. Khmelnitskii, Pis'ma Zh. Eksp. Teor. Fiz. **30**, 248 (1979) [Sov. Phys. JETP Lett. **30**, 248 (1979)].

[2] P. A. Lee and T. V. Ramakrishnan, Rev. Mod. Phys. **57**, 287 (1985).

[3] S. Hikami, A. Larkin, and Y. Nagaoka, Prog. Theor. Phys. **63**, 707 (1980).

[4] S. V. Iordanskii, Yu. B. Lyanda-Geller, and G. E. Pikus, Sov. Phys. JETP Lett. **60**, 206 (1994).

[5] F. G. Pikus and G. E. Pikus, Phys. Rev. B **51**, 16928 (1995).

[6] A. G. Malshukov, K. A. Chao, and M. Willander, Phys. Rev. Lett. **76**, 3794 (1996).

[7] W. Knap, C. Skierbiszewski, A. Zduniak, E. Litwin-Staszewska, D. Bertho, F. Kobbi, J. L. Robert, G. E. Pikus, F. G. Pikus, S. V. Iordanskii, V. Mosser, K. Zekentes, and Y. B. Lyanda-Geller, Phys. Rev. B **53**, 3912 (1996).

[8] A. Zduniak, M. I. Dyakonov, and W. Knap, Phys. Rev. B **56**, 1996 (1997).

[9] T. Hassenkam, S. Pedersen, K. Baklanov, A. Kristensen, C. B. Sorensen, P. E. Lindelof, F. G. Pikus, and G. E. Pikus, Phys. Rev. B **55**, 9298 (1997).

[10] I. V. Gornyi, A. P. Dmitriev, and V. Yu. Kachorovskii, JETP Lett. **68**, 338 (1998).

[11] N. S. Averkiev, L. E. Golub, and G. E. Pikus, Solid State Commun. **107**, 757 (1998); J. Exp. Theor. Phys. **86**, 780 (1998).

[12] S. Pedersen, C. B. Sorensen, A. Kristensen, P. E. Lindelof, L. E. Golub, and N. S. Averkiev, Phys. Rev. B **60**, 4880 (1999).

[13] L. E. Golub and S. Pedersen, Phys. Rev. B **65**, 245311 (2002).

[14] S. A. Studenikin, P. T. Coleridge, N. Ahmed, P. Poole, and A. Sachrajda, Phys. Rev. B **68**, 035317 (2003).

[15] Y. Y. Proskuryakov, A. K. Savchenko, S. S. Safonov, L. Li, M. Pepper, M. Y. Simmons, D. A. Ritchie, E. H. Linfield, and Z. D. Kvon, J. Phys. A: Math. Gen. **36**, 9249 (2003).

[16] I. S. Lyubinskiy and V. Yu. Kachorovskii, Phys. Rev. B **70**, 205335 (2004).

[17] G. M. Minkov, A. V. Germanenko, O. E. Rut, A. A. Sherstobitov, L. E. Golub, B. N. Zvonkov, and M. Willander, Phys. Rev. B **70**, 155323 (2004).

[18] I. S. Lyubinskiy and V. Yu. Kachorovskii, Phys. Rev. Lett. **94**, 076406 (2005).

[19] G. M. Minkov, A. A. Sherstobitov, A. V. Germanenko, O. E. Rut, V. A. Larionova, and B. N. Zvonkov, Phys. Rev. B **71**, 165312 (2005).

[20] L. E. Golub, Phys. Rev. B **71**, 235310 (2005).

[21] M. M. Glazov and L. E. Golub, Fiz. Tech. Poluprov. **40**, 1241 (2006) [Semiconductors **40**, 1209 (2006)].

[22] V. A. Guzenko, M. Akabori, Th. Schäpers, S. Cabañas, T. Sato, T. Suzuki, and S. Yamada, Phys. Status Solidi C **3**, 4227 (2006).

[23] N. Thillosen, Th. Schäpers, N. Kaluza, H. Hardtdegen, and V. A. Guzenko, Appl. Phys. Lett. **88**, 022111 (2006).

[24] D. C. Marinescu, Phys. Rev. Lett. **97**, 176802 (2006).

[25] G. M. Minkov, A. V. Germanenko, O. E. Rut, A. A. Sherstobitov, and B. N. Zvonkov, Phys. Rev. B **75**, 193311 (2007).

[26] V. A. Guzenko, Th. Schäpers, and H. Hardtdegen, Phys. Rev. B **76**, 165301 (2007).

[27] A. E. Belyaev, V. G. Raicheva, A. M. Kurakin, N. Klein, and S. A. Vitusevich, Phys. Rev. B **77**, 035311 (2008).

[28] W. Z. Zhou, T. Lin, L. Y. Shang, L. Sun, K. H. Gao, Y. M. Zhou, G. Yu, N. Tang, K. Han, and B. Shen, J. Appl. Phys. **104**, 053703 (2008).

[29] G. Yu, N. Dai, J. H. Chu, P. J. Poole, and S. A. Studenikin, Phys. Rev. B **78**, 035304 (2008).

[30] M. M. Glazov and L. E. Golub, Phys. Rev. B **77**, 165341 (2008).

[31] F. V. Porubaev and L. E. Golub, Phys. Rev. B **87**, 045306 (2013).

[32] M. Z. Hasan and C. L. Kane, Rev. Mod. Phys. **82**, 3045 (2010).

[33] X.-L. Qi and S.-C. Zhang, Rev. Mod. Phys. **83**, 1057 (2011).

[34] B. A. Bernevig, T. L. Hughes, and S.-C. Zhang, Science **314**, 1757 (2006).

[35] M. König, S. Wiedmann, C. Brüne, A. Roth, H. Buhmann, L. W. Molenkamp, X.-L. Qi, and S.-C. Zhang, Science **318**, 766 (2007).

[36] C. L. Kane and E. J. Mele, Phys. Rev. Lett. **95**, 146802 (2005); **95**, 226801 (2005).

[37] L. Fu and C. L. Kane, Phys. Rev. B **76**, 045302 (2007); L. Fu, C. L. Kane, and E. J. Mele, Phys. Rev. Lett. **98**, 106803 (2007).

[38] D. Hsieh, D. Qian, L. Wray, Y. Xia, Y. S. Hor, R. J. Cava, and M. Z. Hasan, Nature (London) **452**, 7190 (2008).

[39] M. König, H. Buhmann, L. W. Molenkamp, T. Hughes, C.-X. Liu, X.-L. Qi, and S.-C. Zhang, J. Phys. Soc. Jpn. **77**, 031007 (2008); A. Roth, C. Brüne, H. Buhmann, L. W. Molenkamp, J. Maciejko, X.-L. Qi, and S.-C. Zhang, Science **325**, 294 (2009).

[40] C. Liu, T. L. Hughes, X.-L. Qi, K. Wang, and S.-C. Zhang, Phys. Rev. Lett. **100**, 236601 (2008).

[41] I. Knez, Rui-Rui Du, and G. Sullivan, Phys. Rev. Lett. **107**, 136603 (2011); L. Du, I. Knez, G. Sullivan, and Rui-Rui Du, arXiv:1306.1925; I. Knez, C. T. Rettner, See-Hun Yang, S. S. P. Parkin, L. Du, Rui-Rui Du, and G. Sullivan, Phys. Rev. Lett. **112**, 026602 (2014).

[42] P. M. Ostrovsky, I. V. Gornyi, and A. D. Mirlin, Phys. Rev. Lett. **105**, 036803 (2010).

[43] G. Tkachov and E. M. Hankiewicz, Phys. Rev. B **84**, 035444 (2011).

[44] P. M. Ostrovsky, I. V. Gornyi, and A. D. Mirlin, Phys. Rev. B **86**, 125323 (2012).

[45] I. V. Gornyi, V. Yu. Kachorovskii, A. D. Mirlin, and P. M. Ostrovsky, Phys. Status Solidi B (2014), doi:10.1002/pssb.201350309.

[46] V. Krueckl and K. Richter, Semicond. Sci. Technol. **27**, 124006 (2012).

[47] G. Tkachov, Phys. Rev. B **88**, 205404 (2013).

[48] E. McCann, K. Kechedzhi, V. I. Fal'ko, H. Suzuura, T. Ando, and B. L. Altshuler, Phys. Rev. Lett. **97**, 146805 (2006); K. Kechedzhi, E. McCann, V. I. Fal'ko, H. Suzuura, T. Ando, and B. L. Altshuler, Eur. Phys. J. Special Topics **148**, 39 (2007).

[49] I. L. Aleiner and K. B. Efetov, Phys. Rev. Lett. **97**, 236801 (2006).

[50] P. M. Ostrovsky, I. V. Gornyi, and A. D. Mirlin, Phys. Rev. B **74**, 235443 (2006).

[51] M. O. Nestoklon, N. S. Averkiev, and S. A. Tarasenko, Solid State Commun. **151**, 1550 (2011).

[52] V. Krueckl, M. Wimmer, I. Adagideli, J. Kuipers, and K. Richter, Phys. Rev. Lett. **106**, 146801 (2011).

[53] I. Garate and L. Glazman, Phys. Rev. B **86**, 035422 (2012).

[54] E. J. König, P. M. Ostrovsky, I. V. Protopopov, I. V. Gornyi, I. S. Burmistrov, and A. D. Mirlin, Phys. Rev. B **88**, 035106 (2013).

[55] G. M. Minkov, A. V. Germanenko, O. E. Rut, A. A. Sherstobitov, S. A. Dvoretski, and N. N. Mikhailov, Phys. Rev. B **85**, 235312 (2012).

[56] G. M. Minkov, A. V. Germanenko, O. E. Rut, A. A. Sherstobitov, S. A. Dvoretski, and N. N. Mikhailov, Phys. Rev. B **88**, 045323 (2013).

[57] E. B. Olshanetsky, Z. D. Kvon, G. M. Gusev, N. N. Mikhailov, S. A. Dvoretsky, and J. C. Portal, JETP Lett. **91**, 347 (2010); D. A. Kozlov, Z. D. Kvon, N. N. Mikhailov, and S. A. Dvoretsky, *ibid.* **96**, 730 (2013).

[58] M. Mühlbauer, A. Budewitz, B. Büttner, G. Tkachov, E. M. Hankiewicz, C. Brüne, H. Buhmann, and L. W. Molenkamp, Phys. Rev. Lett. **112**, 146803 (2014).

[59] V. M. Gasparyan and A. Yu. Zyuzin, Fiz. Tverd. Tela **27**, 1662 (1985) [Sov. Phys.–Solid State **27**, 999 (1985)].

[60] A. P. Dmitriev, V. Yu. Kachorovskii, and I. V. Gornyi, Phys. Rev. B **56**, 9910 (1997).

[61] D. G. Rothe, R. W. Reinthaler, C.-X. Liu, L. W. Molenkamp, S.-C. Zhang, and E. M. Hankiewicz, New J. Phys. **12**, 065012 (2010).

[62] Here, we implicitly assumed that for a given Fermi energy there is only single value of the Fermi momentum and, consequently, the single value of η (this is the case for HgTe/CdTe wells not too far from the transition point, where the thickness of the quantum well is close to d_c).

[63] S. Chakravarty and A. Schmid, Phys. Rep. **140**, 4 (1986).

[64] C. R. Woods, L. Britnell, A. Eckmann, R. S. Ma, J. C. Lu, H. M. Guo, X. Lin, G. L. Yu, Y. Cao, R. V. Gorbachev, A. V. Kretinin, J. Park, L. A. Ponomarenko, M. I. Katsnelson, Yu. N. Gornostyrev, K. Watanabe, T. Taniguchi, C. Casiraghi, H-J. Gao, A. K. Geim, and K. S. Novoselov, Nat. Phys. **10**, 451 (2014).

[65] In fact, this question is more subtle and the term $N = 1$ requires special attention. It results in an ultraviolet logarithmic divergency (coming from large momenta $q > k_F \gg 1/l$) of the return probability $W(\phi,\phi_0,0)$. This divergency leads to ultraviolet renormalization [49] of the key problem parameters (such as W_0) and will not be discussed here. By default, we assume that all parameters of the problem are already renormalized and that $q \ll k_F$.